

**ESTIMATION AND MAPPING
ABOVE GROUND WOODY
CARBON STOCKS USING LIDAR
DATA AND DIGITAL CAMERA
IMAGERY IN THE HILLY
FORESTS OF GORKHA, NEPAL**

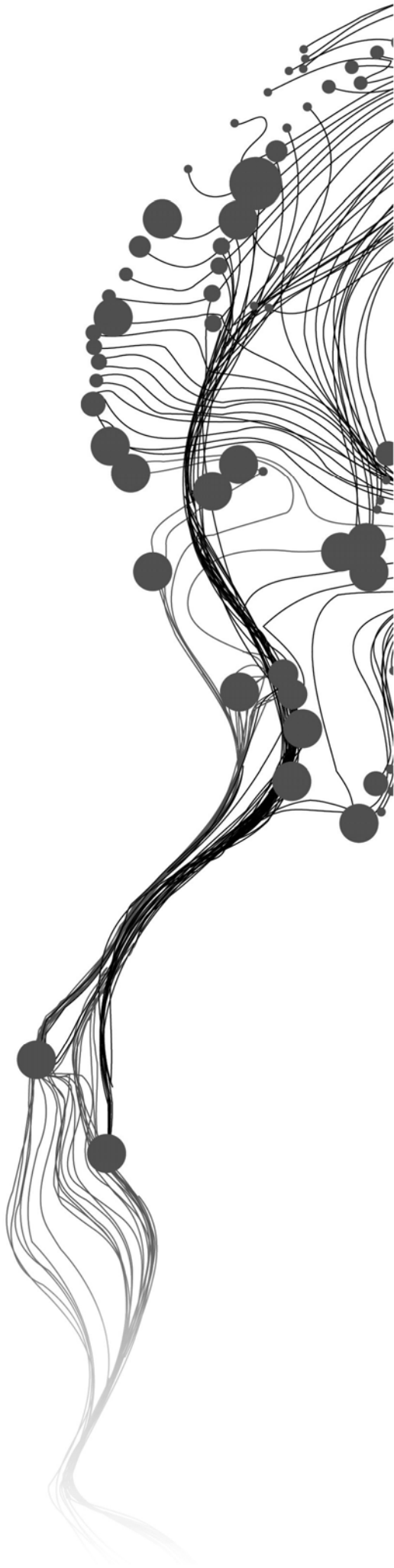
SAJANA MAHARJAN

February, 2012

SUPERVISORS:

Ms. Ir. L.M. van Leeuwen

Dr. Y. A. Hussin



ESTIMATION AND MAPPING ABOVE GROUND WOODY CARBON STOCKS USING LIDAR DATA AND DIGITAL CAMERA IMAGERY IN THE HILLY FORESTS OF GORKHA, NEPAL

SAJANA MAHARJAN

Enschede, The Netherlands, [February, 2012]

Thesis submitted to the Faculty of Geo-Information Science and Earth Observation of the University of Twente in partial fulfilment of the requirements for the degree of Master of Science in Geo-information Science and Earth Observation.

Specialization: Natural Resources Management

SUPERVISORS:

Ms. Ir. L.M. van Leeuwen

Dr. Y. A. Hussin

THESIS ASSESSMENT BOARD:

Dr. A. Voinov (Chair)

Dr.T. Kauranne (External Examiner, Arbonaut Oy Ltd. And Department of Mathematics and Physics - Lappeenranta University of Technology, Finland)

DISCLAIMER

This document describes work undertaken as part of a programme of study at the Faculty of Geo-Information Science and Earth Observation of the University of Twente. All views and opinions expressed therein remain the sole responsibility of the author, and do not necessarily represent those of the Faculty.

ABSTRACT

There is a demand for methods to accurately estimate above ground carbon stock as Kyoto Protocol needs reporting on carbon stock and stock changes. This study describes development of a method to accurately estimate and map above ground woody carbon stocks using airborne LIDAR data with an average point density of 0.8 point/m² and high resolution (0.45 m) Digital Camera imagery in the hilly forests of Gorkha, Nepal. The study aims to develop a method for tree crown delineation using airborne LIDAR data and high resolution Digital Camera imagery and to analyse potential of LIDAR data in separating intermingled trees. In addition, models were developed using obtained biophysical parameters (CPA and height) for carbon stocks estimation and mapping.

Digital Surface Model (DSM) was generated using LIDAR first return and Digital Terrain Model (DTM) was generated using only ground points. Canopy Height Model (CHM) was computed as the difference between DSM and DTM. RMSE of 2.8 m was obtained for LIDAR derived height. Tree crown delineation was done using region growing approach in object based image analysis (OBIA). Overall segmentation accuracy was 76.2% based on 1:1 correspondence. The delineated crowns were classified into two classes (*Shorea robusta* and others) using nearest neighbour classification. The overall accuracy of the classification was 75.86%.

Above ground biomass (AGB) was calculated using allometric equation from DBH and height measured in the field which was then converted into carbon stock using a conversion factor of 0.47. Linear regression models were applied to derive the relation of carbon with CPA, height and a combination of both CPA and height. All models were significant at 95% confidence level and the lowest RMSE% of 36.8% (*Shorea robusta*) and 32.4% (others) were obtained from multiple regression models. Multicollinearity was low, so it had no effect on the model. The results indicate that the estimation of above ground carbon stock improves using two variables (CPA and height) than using either of the variables alone. Multiple regression models were used to estimate carbon stocks of the study area. The total amount of carbon stocks in the study area was approximately 89.45 MgCha⁻¹.

Keywords: LIDAR, Digital Camera Imagery, Segmentation, Classification, Carbon stock, Crown projection area, Height, Model

ACKNOWLEDGEMENTS

I am sincerely grateful to the Netherlands Government and the Netherlands organisation for international cooperation in higher education (NUFFIC) for granting me a scholarship to study in the Netherlands without which this study was not possible.

I would like to express my sincere gratitude and appreciation to my first supervisor, Ms. Ir. L.M. Louise van Leeuwen for her guidance, suggestions, comments and encouragement from the beginning till the completion of this research and for bringing ideas to shape up my work. I would like to thank my second supervisor, Dr. Yousif Hussin for his valuable suggestions and motivation. I would like to thank Dr. Alexey Voinov for his comments and suggestions during my proposal defense and mid-term which help to improve my work.

A special gratitude to my course director Dr. Michael Weir and his NRM team for the efficient management of this course. I am thankful to ITC who gave me a good academic environment to learn many new skills and techniques of GIS and Remote Sensing which is my major achievement of my life.

I would like to acknowledge ICIMOD, ANSAB and FECOFUN for their support in the arrangement of the fieldwork and other technical support. I am thankful to FRA Nepal for providing LIDAR data and Digital Camera imagery for this research.

I would like to thank Basanta Gautam of Arbonaut of Finland, Khamarrul Azahari Razak, Dr. David Rossiter and Dr. Kourosh Khoshelham for sharing their knowledge and concept which help me to clear my ideas during the research.

I am thankful to all my friends of ITC. Special thanks to Nguyet and Pema for data collection during the fieldwork. Special thanks to Nepali Samaj who really keep homely environment, support and refreshment during the entire course.

Finally, I am indebted to my family and want to dedicate my thesis to my mother. I would like to thank my brothers Sudarshan and Sushan for their support during my study.

Sajana Maharjan
Enschede, The Netherlands
February, 2012

TABLE OF CONTENTS

Abstract	i
Acknowledgements	ii
List of figures	vi
List of tables.....	vii
List of acronyms	viii
1. INTRODUCTION.....	1
1.1. Background	1
1.2. Overview of application of remote sensing for biomass estimation	3
1.3. Rationale and problem statement.....	4
1.4. Research objectives.....	5
1.5. Theoretical framework of research	5
1.6. Concepts and Definitions	6
1.6.1. LIDAR and its principle	6
1.6.2. Point cloud.....	7
1.6.3. Crown Projection Area	8
1.6.4. Community Forest.....	8
1.6.5. Intermingled trees	8
2. STUDY AREA	9
2.1. Criteria for study area selection	9
2.2. Overview of the study area.....	9
2.2.1. Socio-economic information and demography.....	10
2.2.2. Topography.....	10
2.2.3. Climate.....	10
2.2.4. Temperature.....	10
2.2.5. Rainfall.....	11
2.2.6. Vegetation	11
3. MATERIALS AND METHODS	13
3.1. Data Used.....	13
3.1.1. Digital Camera Imagery	13
3.1.2. LIDAR data	13
3.1.3. Maps.....	13
3.1.4. Software.....	13
3.1.5. Field Equipment	13
3.2. Image pre-processing.....	14
3.2.1. Image filtering.....	14
3.3. Research Method.....	14

3.3.1.	Field work	15
3.3.2.	Fieldwork data analysis	17
3.3.3.	Manual delineation of trees	17
3.3.4.	CHM (Canopy Height Model) Preparation.....	17
3.3.5.	Accuracy assessment of LIDAR derived height.....	17
3.3.6.	Tree crown delineation	18
3.3.7.	Accuracy assessment of tree crown delineation	21
3.3.8.	Segmentation assessment for intermingled trees.....	22
3.3.9.	Image classification.....	22
3.3.10.	Classification accuracy assessment.....	22
3.3.11.	Above Ground Biomass and Carbon Stock calculation.....	22
3.3.12.	Regression analysis and model validation.....	23
3.3.13.	Carbon stock mapping.....	23
4.	RESULTS	25
4.1.	Descriptive analysis of the field data	25
4.2.	CHM preparation and accuracy assessment of LIDAR derived height.....	27
4.3.	Tree crown delineation and accuracy assessment.....	28
4.4.	Image classification and accuracy assessment	29
4.5.	LIDAR data in separating intermingled tree crowns	30
4.6.	Model development and validation.....	30
4.6.1.	Relationship between CPA and Carbon	30
4.6.2.	Relationship between height and Carbon.....	31
4.6.3.	Relationship of Carbon with CPA and height	32
4.6.4.	Model validation	32
4.7.	Carbon Stock mapping	34
5.	DISCUSSION.....	35
5.1.	CHM preparation and accuracy assessment of LIDAR derived height.....	35
5.2.	Tree crown delineation and accuracy assessment.....	36
5.3.	Image classification and accuracy assessment	37
5.4.	LIDAR data in separating intermingled tree crowns	38
5.5.	Model development and validation.....	39
5.6.	Biomass and carbon stock estimation	40
5.7.	Sources of error or uncertainties	41
5.7.1.	Allometric equation.....	41
5.7.2.	Unsystematic shift between LIDAR data and Digital camera imagery.....	41
5.7.3.	Other errors/uncertainty.....	41

6.	CONCLUSIONS AND RECOMMENDATIONS	43
6.1.	Conclusions	43
6.2.	Recommendations	44
	List of references	45
	Appendices	49

LIST OF FIGURES

Figure 1.1: Theoretical framework of the research.....	6
Figure 1.2: Typical operation of an airborne LIDAR survey, source: (Heritage et al., 2009).....	7
Figure 1.3: Point cloud (change in colour shows height variation of the object).....	8
Figure 1.4: Crown Projection Area, source: (Gschwantner et al., 2009).....	8
Figure 2.1: Study area, Gorkha, Nepal, (a) Nepal map (b) Ludikhola watershed (c) Selected CFs for the study.....	10
Figure 3.1: Flowchart of research method.....	15
Figure 3.2: Chessboard segmentation.....	18
Figure 3.3: Radiometric ‘topography’ of subset of VHR image of forest, source: (Culvenor, 2002).....	19
Figure 3.4: Steps for tree crown delineation.....	20
Figure 3.5: Different conditions of 1:1 correspondence, source: (Zhan et al., 2005).....	21
Figure 4.1: Tree species occurrence in the study area.....	25
Figure 4.2: DBH and height of the major tree species.....	26
Figure 4.3: Number of intermingled trees.....	26
Figure 4.4: (a) DSM and (b) DTM derived from point cloud.....	27
Figure 4.5: CHM of the study area.....	27
Figure 4.6: LIDAR derived tree height compared with field measured tree height.....	27
Figure 4.7: Tree crown delineation using region growing approach.....	28
Figure 4.8: Tree species map of the study area in Ludikhola watershed, Gorkha, Nepal.....	29
Figure 4.9: No separation of intermingled trees.....	30
Figure 4.10: Relationship between CPA and carbon.....	31
Figure 4.11: Relationship between height and carbon.....	32
Figure 4.12: Scatterplots of predicted versus observed carbon.....	33
Figure 4.13: Carbon stock map of the study area and inset shows the details of carbon stock per tree.....	34
Figure 5.1: Crowns shape (a) coniferous tree (b) deciduous tree.....	35
Figure 5.2: Digital camera image showing shadow area and segments on the shadow area.....	36
Figure 5.3: Example of commission and omission error.....	37
Figure 5.4: Distortion in digital camera image.....	37
Figure 5.5: Showing multipoint (from point cloud) (red oval shapes show 2 trees that are intermingled).....	38
Figure 5.6: Different degree of two intermingled canopy trees.....	39
Figure 5.7: Sources of errors and their accumulation and propagation into the map.....	42

LIST OF TABLES

Table 3:1: Softwares used in the research.....	13
Table 3:2: List of equipments used for the field work.....	14
Table 3:3: Plot number in each stratum for data collection.....	16
Table 4:1: Forest inventory	25
Table 4:2: 1:1 Correspondence of reference and segmented CPA.....	29
Table 4:3: Accuracy assessment of tree species classification	30
Table 4:4: Regression analysis of <i>Shorea robusta</i> and other species	31
Table 4:5: Regression analysis of <i>Shorea robusta</i> and other species.....	31
Table 4:6: Multiple linear regression using height, CPA and carbon	32

LIST OF ACRONYMS

AGB	Above Ground Biomass
ALS	Airborne Laser Scanning
AVHRR	Advanced Very High Resolution Radiometer
AGL	Above Ground Level
ANOVA	Analysis of Variance
ANSAB	Asia Network for Sustainable Agriculture and Bio-resources
CF	Community Forest
CFUG	Community Forest User Group
CHM	Canopy Height Model
CPA	Crown Projection Area
DBH	Diameter at Breast Height
DCM	Digital Canopy model
DFO	District Forest office
DSCO	District Soil Conservation office
DSM	Digital Surface Model
DTM	Digital Terrain Model
FCPF	Forest Carbon Partnership Facility
FECOFUN	Federation of Community Forest Users' Nepal
FRA	Forest Research Assessment
GPS	Global Positioning System
ICIMOD	International Centre for Integrated Mountain Development
IMU	Inertial Measurement Unit
INU	Inertial Navigation Unit
IPCC	International Panel on Climate Change
LIDAR	Light Detection and ranging
MODIS	Moderate resolution Imaging Spectroradiometer
MPFSN	Master Plan for the Forestry Sector Nepal
NOAA	National Oceanic and Atmospheric Administration
OBIA	Object Based Image Analysis
R ²	Coefficient of determination
Radar	Radio detection and Ranging
REDD	Reducing Emissions from Deforestation and Forest Degradation
RMSE	Root Mean Square Error
R-PP	Readiness Preparation Proposal
TIN	Triangulated Irregular Network
UNEP	United Nations Environment Programme
UNFCCC	United Nations Framework Convention on Climate Change
VHR	Very High Resolution
VIF	Variation Inflation Factor

1. INTRODUCTION

1.1. Background

Carbon dioxide (CO₂) is one of the most important greenhouse gases (IPCC, 2007) and increased concentration of this gas is one of the likely causes of climate change. CO₂ also occurs from natural sources in a natural situation without anthropogenic influences. Animal and plant respiration process releases CO₂ in the atmosphere. On the other hand, Atmospheric CO₂ is assimilated during photosynthesis and carbohydrates are formed which are building blocks of vegetation. Then, a lot of carbon is stored in vegetation. Therefore, there is almost balance between the natural CO₂ emissions and removals from the entire carbon cycle (U.S. EPA, 2011). However, the natural carbon cycle is being disturbed due to human activities mainly due to fossil fuel use and land use change/deforestation resulting to the increase in atmospheric concentrations of CO₂.

Forests are large pools of carbon. They act as carbon sinks but can also be sources of CO₂ emission into the atmosphere, therefore they play a crucial role in the global carbon cycle (Muukkonen et al., 2007). At a global scale, forests hold more than 60% of the carbon contained in the aboveground biomass and about 45% of the carbon contained in soils, roots and litter (Dixon et al., 1993). On the other hand, approximately 18% of global biomass carbon emission per year is from forest fire (UNEP, 1999). Forest fires emit carbon in a very short period of high concentration whereas deforestation emits carbon through a longer process. Therefore, increasing afforestation, reforestation and reducing deforestation are mitigation measures for global climate change (Hunt, 2009). This implies that it is necessary to maintain existing forests as well as increase forest areas.

The United Nations Framework Convention on Climate Change (UNFCCC) and the Kyoto Protocol are the two important international agreements, which address the issue of reducing anthropogenic greenhouse gas (GHG) emissions in the atmosphere. UNFCCC is a framework convention under which activities take place and agreements are made. Kyoto Protocol, Bali Action Plan and recently Durban climate change conference are some of the agreements under UNFCCC. Although UNFCCC does not explicitly stipulate levels to which Parties have to reduce their GHG emissions (Patenaude et al., 2005), it has adopted Kyoto Protocol on 11 December 1997 which requires signatory countries to reduce human-induced emissions of CO₂ by an average of five percent below their emission level of 1990 by 2008-2012 (UNFCCC, 1997). Signatory countries are given the option to meet part of their reduction requirements through conservation and enhancement of the carbon stored in forest ecosystems. For this, they have to estimate carbon stocks for 1990 as a baseline and report any changes since 1990 from all deforestation, reforestation and afforestation activities.

In order to enable full, effective and sustained implementation of the convention, the Bali Action Plan (UNFCCC, 2007) considered Reducing Emissions from Deforestation and Forest Degradation (REDD) as an important climate change mitigation action. It opened opportunities for developing countries to participate in forest carbon financing through the REDD mechanism (MOFSC, 2009a). According to the REDD mechanism, industrialized countries are allowed to offset their emissions by purchasing carbon credits from developing countries, which reduce emissions from deforestation and forest degradation by avoiding such activities (Dhital, 2009). This emerging mechanism will compensate to the developing countries for their forest conservation and regeneration effort (Acharya et al., 2009).

REDD is an opportunity for developing countries including Nepal to contribute significantly to emission reduction efforts under international climate regime (Oli et al., 2009). Approximately 40% of the total land area of Nepal is covered with forests (DFRS, 1999). This indicates that Nepal is potentially a carbon sink. Nepal being a UNFCCC signatory and a member of REDD program has recently submitted the Readiness Preparation Proposal (R-PP) to participate in the Forest Carbon Partnership Facility (FCPF)(MOFSC, 2009b). Nepal has to present the country's current status of carbon stored in the forest and emitted from deforestation and forest degradation in order to participate in carbon finance mechanism. Thus, reliable baseline statistics on national forest carbon stocks and sources of carbon emission is required to establish a national reference scenario and to implement REDD strategy. However, Nepal does not have statistics on any carbon stock of above or below ground biomass. Remote sensing can be used for assessment of above ground carbon in all land covers. Forest is the major carbon sink and advanced remote sensing technology can be applied for carbon estimation (Oli et al., 2009). Therefore, REDD implementation, it is necessary to develop a method which can accurately estimate forest above ground biomass (AGB) and carbon stocks at national level.

“Above ground biomass is the total amount of biological material (usually oven-dried to remove water) present above the soil surface in a specified area” (Drake et al., 2003) and carbon is approximately 47% of the AGB (IPCC, 2003). Conventional methods for biomass estimation are based on field measurements and they are time consuming and expensive (García et al., 2010). Thus, these methods are not practical for regional or national scale. There are remote sensing methods available to estimate carbon stocks from local level to national level but these methods too cannot measure carbon stocks directly and thus require additional ground-based data collection (Drake et al., 2003). Although both methods need field measurements, conventional methods (destructive sampling) are limited in terms of spatial and temporal sampling as they are time consuming and labour intensive whereas remote sensing provides detailed and spatially explicit information on forest biomass at a wide range of spatial and temporal scale (García et al., 2010). However, appropriate method is required to extract relevant data from it. Tree parameters such as crown area can be obtained from the remote-sensing measurements and forest attributes such as DBH and height can be obtained from ground based measurements. Then, the obtained forest attributes from ground based and remote-sensing measurements can be converted into estimates of carbon stocks using allometric equation.

Allometric equations are quantitative relationships between an easily measured independent variable such as diameter at breast height (DBH) and height and another difficult to assess component like biomass that provides relatively accurate estimates (Phillips et al., 2002). DBH is the stem diameter of a tree at 1.3 m above the ground level (FAO, 2004b). DBH and height are the important tree parameters for biomass estimation (Jenkins et al., 2003). Since DBH can be more easily measured than height, most of the allometric equations are developed based on the DBH (Jenkins et al., 2003; Tritton et al., 1982). However, Ketterings et al. (2001) use DBH and height to develop a site specific allometric equation for biomass estimation that is applicable for trees with DBH of 8-48 cm. The study was done in mixed secondary forests of Sumatra, Indonesia and the standard errors for the parameters 'a' and 'b' of the developed equation were 0.021 and 0.106 respectively.

High resolution aerial photographs such as Digital Camera imagery are a source for biomass estimation as it gives crown area and tree species information (Massada et al., 2006). Individual tree crown can be delineated using high resolution (<1 m) Digital Camera imagery (Leckie et al., 2003). This is particularly interesting because several studies (Hirata et al., 2009; Shimano, 1997) have proved that there is a relation between crown projection area (CPA) and DBH. Thus, if CPA can be obtained from the satellite images and aerial photographs, DBH can be calculated for these respective trees. Then, biomass can be calculated

using an allometric equation. However, this approach does not include height. Various remote sensing approaches for carbon estimation have been reviewed by Patenaude et al. (2005) who concluded that LIDAR (Light Detection and Ranging) techniques are promising for carbon stocks estimation. LIDAR provides height of the target as it sends out the pulse of laser light to the target and records both the travel time of the laser and the energy (intensity) that is scattered back from the target, thus providing distance from the sensor to the target (Dubayah et al., 2000). LIDAR instruments have shown the capability to accurately estimate forest structural characteristics such as canopy heights, stand volume, basal area and above ground biomass (Dubayah et al., 2000). Although LIDAR does not penetrate cloud, it has the unique capability to measure three dimensional vertical structure of vegetation (Song et al., 2010).

1.2. Overview of application of remote sensing for biomass estimation

There are several studies done to estimate forest AGB using remote sensing data. For the global, continental and national scale, the coarse spatial resolution optical sensors such as NOAA AVHRR (Dong et al., 2003) and MODIS (Baccini et al., 2004) have been useful for estimating biomass because of spatial resolution, image coverage and high frequency in data acquisition (Lu, 2006). For regional and at local scale, medium resolution satellite imagery such as Landsat TM is required to estimate forest AGB. However, data saturation problem was found by Steininger (2000) when forest AGB reached about 15 kg/m² for Landsat TM satellite imagery. Forest AGB estimation for large areas using coarse spatial resolution data has been limited because of mixed pixels and the huge difference between the support of ground reference data and pixel size of the satellite data (Muukkonen et al., 2007). In addition, Thenkabail et al. (2004) found that optical sensors such as Landsat, AVHRR and MODIS cannot yet be used for estimation of carbon stocks of tropical forests with certainty. Satellite based vegetation indices (Lu et al., 2004) are also used for ABG estimation. Nevertheless, this method underestimates carbon stocks in the tropical forest since optical sensors are less effective in the dense canopy of the forest (Gibbs et al., 2007).

Very high resolution (VHR) images with spatial resolutions of less than 5m (Lu, 2006) such as aerial photograph, satellite images such as Quickbird, IKONOS, WorldView and Geoeye images can detect individual tree crowns (Gonzalez et al., 2010). Using high resolution data, various operations like tree crown delineation, species identification and crown density estimation have been done (Katoh et al., 2009). However, canopy illumination and topography cause high spectral variation and shadows which may create difficulty in AGB estimation (Lu, 2006). Several studies have done using VHR satellite images to develop methods for carbon estimation of the forest. In this context, Shrestha (2011) determined relationship between AGB and CPA using VHR Geoeye image for carbon estimation. In addition, Jamarkattel (2011) developed a method determining relationship between AGB and CPA to estimate the carbon stock using Geoeye and Worldview images. However, extraction of forest information such as crown area from VHR imagery is difficult using pixel based approach. Therefore, object-oriented approach is being used to analyse VHR imagery.

Object oriented approach is also called object based classification (Zhang et al., 2010). In VHR imagery, pixel size is very small compared to the target entity such as a tree crown (Song et al., 2010). Thus, a group of pixels is combined to represent target entity. Traditional pixel based classification is not suitable for VHR images because the image contains too much detail and will get a pepper and salt noise (Ke et al., 2010) because pixel values differ slightly even within one feature. As alternative to this traditional approach, object-oriented approach has been widely used for VHR images. The basic units of object-oriented approach are image objects that are generated when spatially adjacent pixels are clustered based on homogeneity criteria (Ke et al., 2010). Object-oriented classification has been successfully applied for forest species classification using VHR imagery (Jamarkattel, 2011; Ke et al., 2010; Tsendbazar, 2011).

Object-oriented classification uses not only spectral information but also other information such as shape, texture and contextual relationships.

1.3. Rationale and problem statement

Biomass of a tree is equal to the product of volume and wood density (Ketterings et al., 2001). DBH and height of the tree are the parameters for volume calculation. In order to get the accurate volume and then biomass of a tree, it is crucial to include these tree parameters. Using satellite images and other aerial photographs, these parameters cannot be retrieved directly. However, CPA of trees can be obtained from the VHR images. There are studies done which show there is relationship between CPA and DBH (Hirata et al., 2009; Song et al., 2010). Then, biomass can be calculated using CPA and DBH from the regression model. However, models developed based on just CPA and DBH may not give sufficiently accurate estimate of biomass because these models do not include height of the trees. Trees with same DBH may differ in height and this will vary in biomass. Thus, to get the accurate estimate of biomass, height should also be included. It is difficult to measure tree height accurately in the forest from the current manual photogrammetric or field survey techniques (Popescu et al., 2004) and height information cannot be obtained from optical remote sensing data. To overcome this, LIDAR technique is used as it gives height of the trees. While CPA and height can now be obtained, DBH or biomass cannot be obtained directly from high resolution satellite images or LIDAR data. However, a relationship between CPA, tree height and biomass may be developed for accurate carbon stocks estimation through regression analysis. Since, two independent variables i.e. CPA and height will be used for biomass estimation, it is necessary to check multicollinearity between these variables.

CPA is obtained from tree crown delineation. Tree crown delineation is important step in biomass estimation because based on the obtained CPA, tree species classification and models are developed to estimate biomass. Several studies have been done for tree crown delineation using high resolution images (Jamarkattel, 2011; Tsendbazar, 2011). However, to accurately estimate biomass, better tree crown delineation is required. In addition to spectral reflectance information, this research is adding height information. With this information, it is expected to improve tree crown delineation. In addition, tree height can vary between species and within species. This is expected to help in recognizing individual tree and species recognition. Each species has different wood density resulting in variation in carbon storage in the tree. Therefore, it is crucial to recognize the tree species. Once individual tree and species is recognized then, species specific allometric equation can be used.

Information about individual tree species can be obtained from VHR multispectral imagery (Leckie et al., 2003). VHR imagery provides opportunity to differentiate tree species (Ke et al., 2010). However, crown of intermingled trees cannot be separated using satellite images, which causes error in biomass estimation (Hirata et al., 2009; Palace et al., 2008). However, if the intermingled trees are homogenous in species composition, this might affect less to the AGB estimation because wood density is the same. LIDAR data may be able to separate intermingled tree crowns based on their tree tops as it gives tree height.

Approaches using integration of aerial photograph and canopy height model (CHM) derived from LIDAR data are expected to give better results for forest AGB estimation than using either aerial photograph or LIDAR data alone (Popescu, 2007). Kim et al. (2010) found that the integration of LIDAR data (5-10 points/m²) and aerial photograph gives better segmentation result. Leckie et al. (2003) stated that both LIDAR and spectral based tree delineation can lead to the close estimate of crown size. A review of literatures (Chen et al., 2005; Kim et al., 2010; Popescu et al., 2004) on integration of airborne LIDAR data and multispectral data provides an accurate measurement of AGB in the various forest biomes. This

is because of improvement in feature extraction task i.e. improvement in segmentation. Moreover, Ke et al. (2010) found that the integration of both spectral and airborne LIDAR data resulted in more accurate tree species classification than using either of the data alone. Therefore, in order to improve the assessment of carbon stocks, integration of LIDAR data with Digital Camera imagery is an appropriate approach as it gives information on both the crown area of individual tree and tree height.

This research aims to develop a method integrating LIDAR data (0.8 point/m² on average) with VHR Digital Camera imagery (0.45 m resolution). Generally LIDAR with high point density closely reflects the shape of the tree. But this research is using low point density because this is cheaper compared to high point density LIDAR data.

Apart from aforementioned, Nepal being a UNFCCC signatory and a member of REDD program, reliable baseline statistics on national forest carbon stocks is required. Thus, this research will fill the gap that remains in the scientific domain of estimating carbon of forest AGB with improvement in the assessment.

1.4. Research objectives

The main objective of this research is to develop a method to accurately estimate and map above ground woody carbon stocks using airborne LIDAR data and high resolution Digital Camera imagery in the hilly forests of Gorkha, Nepal.

The specific objectives

- i. To develop a method for tree crown delineation by integrating airborne LIDAR data with high resolution Digital Camera imagery
- ii. To analyse the potential of LIDAR data in separating intermingled tree crowns
- iii. To develop and compare the accuracy of the model for carbon and CPA; carbon and height; carbon, CPA and height
- iv. To estimate and map the amount of above ground woody carbon stocks (as carbon stock hereafter) in the study area

Research Questions

- i. What is the accuracy of tree crown delineation using LIDAR data and Digital Camera imagery?
- ii. How effective is LIDAR data in separating intermingled tree crowns?
- iii. Is there any multicollinearity between CPA and height?
- iv. Which model has the highest accuracy for carbon estimation?
- v. What is the amount of carbon stock in the study area?

Hypothesis

- i. Tree crown delineation can be done with more than 70% accuracy using airborne LIDAR data and high resolution Digital Camera imagery.
- ii. There is multicollinearity between CPA and height.
- iii. Model developed including both height and CPA improves the accuracy of carbon estimation compared to the model including only CPA and the model including only height.

1.5. Theoretical framework of research

The research began with literature review and problem identification. Based on the identified problem, objectives were defined and research questions were formulated. Data required for the research were

identified and field work was carried out. LIDAR data, Digital Camera imagery and field data were analysed. The obtained results were discussed and conclusions were drawn. The process is shown in Figure 1.1.

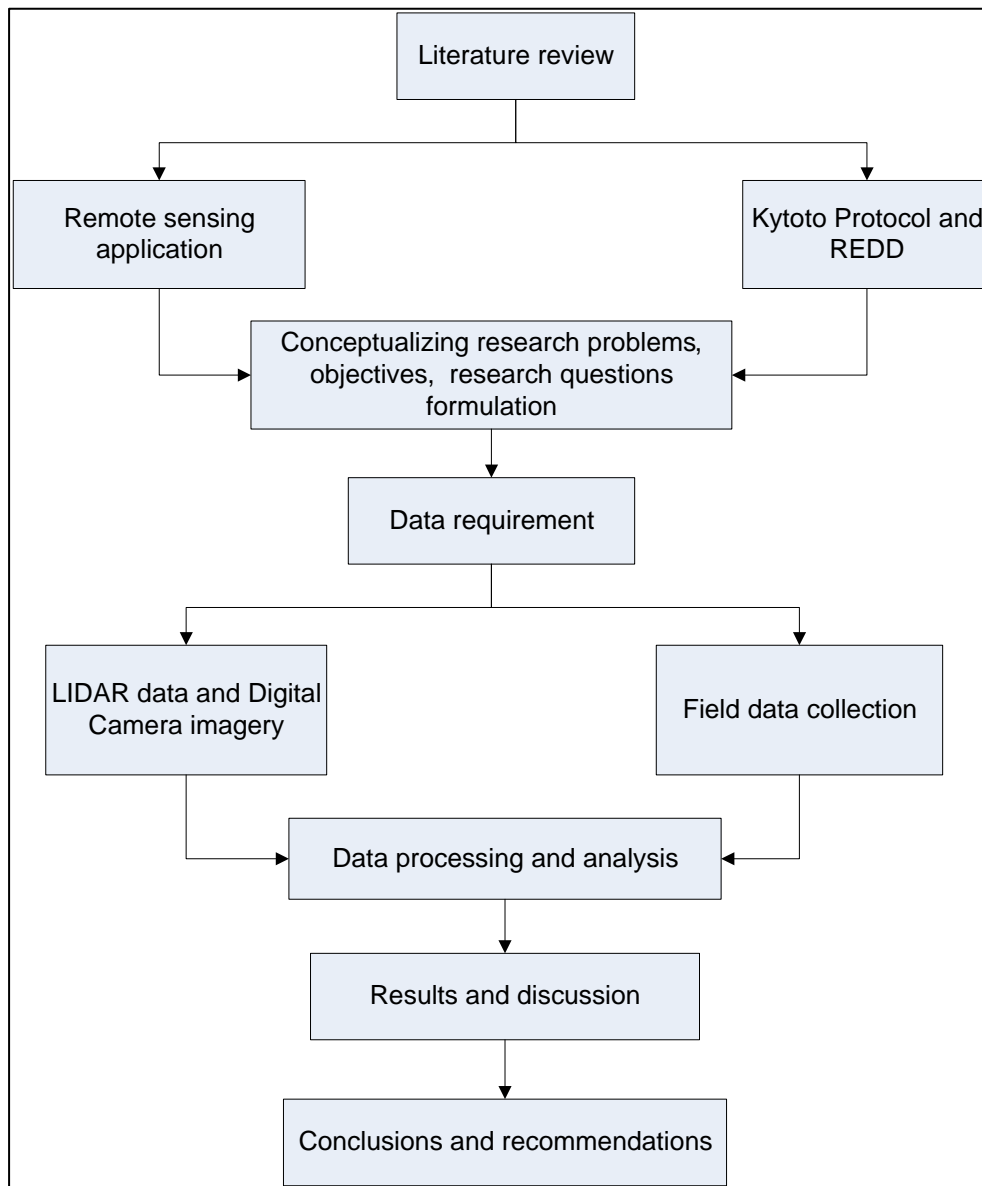


Figure 1.1: Theoretical framework of the research

1.6. Concepts and Definitions

1.6.1. LIDAR and its principle

In the recent years, researchers are actively involved in estimation of AGB using LIDAR technology. LIDAR is a promising technology that can measure the height of the trees and provide highly accurate estimates of AGB (Lefsky et al., 2002). In addition, Kim et al. (2010) stated that AGB of the forest and its carbon storage can be effectively estimated using aerial photograph and LIDAR data.

LIDAR is one of the active remote sensing techniques that have ability to capture 3-dimensional measurements over the large areas. LIDAR is also called airborne laser scanning (ALS). LIDAR system

consists of (i) the LIDAR sensor which sends out the pulse of laser light to the target and records both the travel time of the laser and the energy (intensity) that is scattered back from the target (Dubayah et al., 2000) (ii) the Inertial Navigation Unit (INU) also called Inertial Measurement Unit (IMU) of the aircraft and (iii) GPS (Heritage et al., 2009). In order to correct the pitch, roll and yaw of the aircraft, INU is used in the system so that LIDAR measurements are corrected. Using differential GPS, accurate x, y, z position of sensor is obtained relative to ground-based GPS base stations. The co-ordinates of the reflecting object can be calculated by knowing the sensor position, the distance and incidence angle of each measurement (Hyypä et al., 2000). Operation of an airborne LIDAR surveys are given in Figure 1.2.

Airborne LIDAR system is useful for directly assessing vegetation characteristics because of its features such as extensive area coverage, high sampling intensity, ability to penetrate beneath the top layer of the canopy, precise geolocation and accurate ranging measurements (Popescu et al., 2004). In addition, there is no saturation problem at high biomass levels (Patenaude et al., 2005). Nevertheless accurate and precise product of LIDAR data depends on its point density (Heritage et al., 2009). Point density for airborne LIDAR is the number of laser echoes (returns) per unit area. It can be considered as equivalent to the resolution for passive imaging sensors.

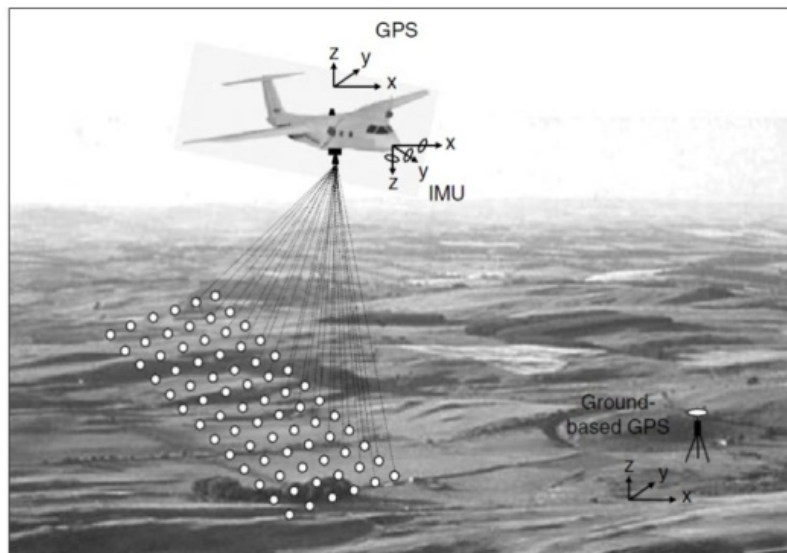


Figure 1.2: Typical operation of an airborne LIDAR survey, source: (Heritage et al., 2009)

LIDAR systems for forestry application can be categorized based on two characteristics: (1) record of return signal (2) size of footprint. Based on first characteristics, LIDAR systems can be divided into discrete return LIDAR system (records single or multiple returns for each pulse) and full waveform LIDAR system (records the amount of energy returned to the sensor for a series of equal time intervals)(Lim et al., 2003). Based on second characteristics, LIDAR systems can be divided into small footprint systems which record footprint with a diameter of up to 100 cm and large footprint systems which record footprint in the size range 10-100 m (Heritage et al., 2009).

1.6.2. Point cloud

Point cloud is the output of airborne laser scanner which is a cloud of geometrically unstructured observations consisting of a large number of individual measurements in three dimensions (Heritage et al., 2009) as shown in Figure 1.3.

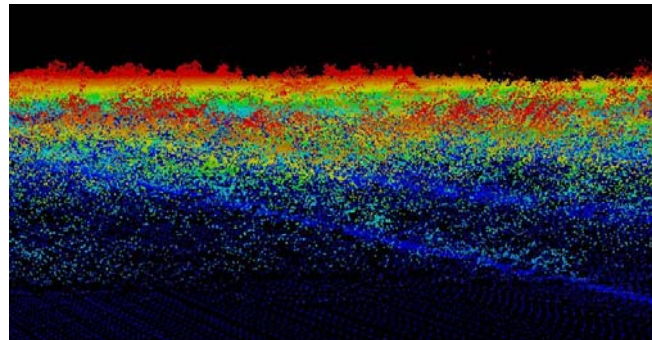


Figure 1.3: Point cloud (change in colour shows height variation of the object)

1.6.3. Crown Projection Area

Crown projection area is defined as the area of the vertical projection of the outermost perimeter of the tree crown on the forest floor (Gschwantner et al., 2009) as shown in Figure 1.4. It is an important variable for estimating forest above ground biomass using remotely sensed images.

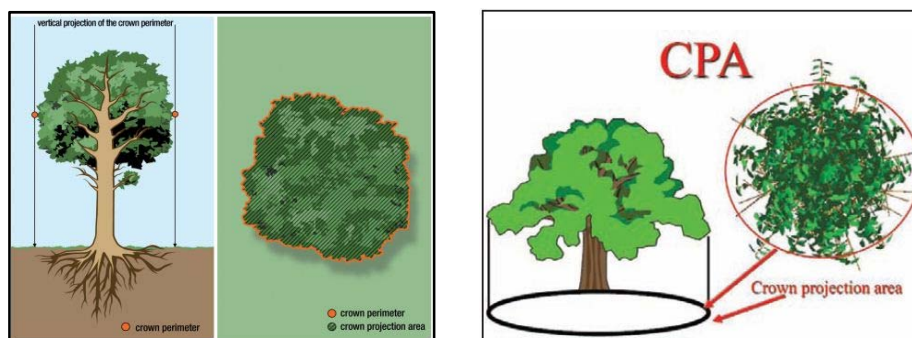


Figure 1.4: Crown Projection Area, source: (Gschwantner et al., 2009)

1.6.4. Community Forest

Community forest (CF) is the national forest which is legally handed over to the local people for their development, conservation and use (Yadav, 2004). From the local people, community forest user group (CFUG) is being developed in the community to carry out activities for the protection and sustainable management of the forest resources. The user group members participate in the decision making processes and implement the CF activities based on their constitution and operational plan. Constitution and operational plan of CFUG are being formulated with the support of a forest technician.

1.6.5. Intermingled trees

According to the Oxford English Dictionary, intermingle means to mix together. When the branches or canopy of two or more trees mix together, the trees are called intermingled.

2. STUDY AREA

2.1. Criteria for study area selection

The study area was selected taking following criteria under consideration.

- **Implementation of REDD+ pilot project**

For the implementation of the REDD+ pilot project, it was being piloted in three watersheds. Ludikhola watershed was one of the pilot sites and this watershed was selected as representative of sub-tropical forests of Nepal.

- **Accessibility and availability of data**

The study area was selected considering accessibility as the research should be carried out within limited budget and time. LIDAR data and Digital Camera imagery was available for this watershed as it was pilot project site.

2.2. Overview of the study area

Ludikhola watershed lies in the Gorkha district of western development region of Nepal. It lies in the southern part of the Gorkha, district and is located between 27°55'02"-27°59'43"N latitude and 84°33'23"-84°40'41"E longitude. It covers forest area of 1888 ha ranging from 318 m to 1714 m a.m.s.l. (ICIMOD et al., 2010; REDD, 2011) altitude having sub-tropical forests. The watershed was heavily deforested in the past and this has been controlled through community forest management.

There are 31 community forest (CF) in the Ludikhola watershed. The study was carried out only in five CF (Ludidamgade, Birenchok, Kuwadi, Chisapani and Shikhar). It was not conducted in all CFs because of time and software limitation. eCognition software (for segmentation) cannot process the whole image of the watershed. The study area is shown in Figure 2.1.

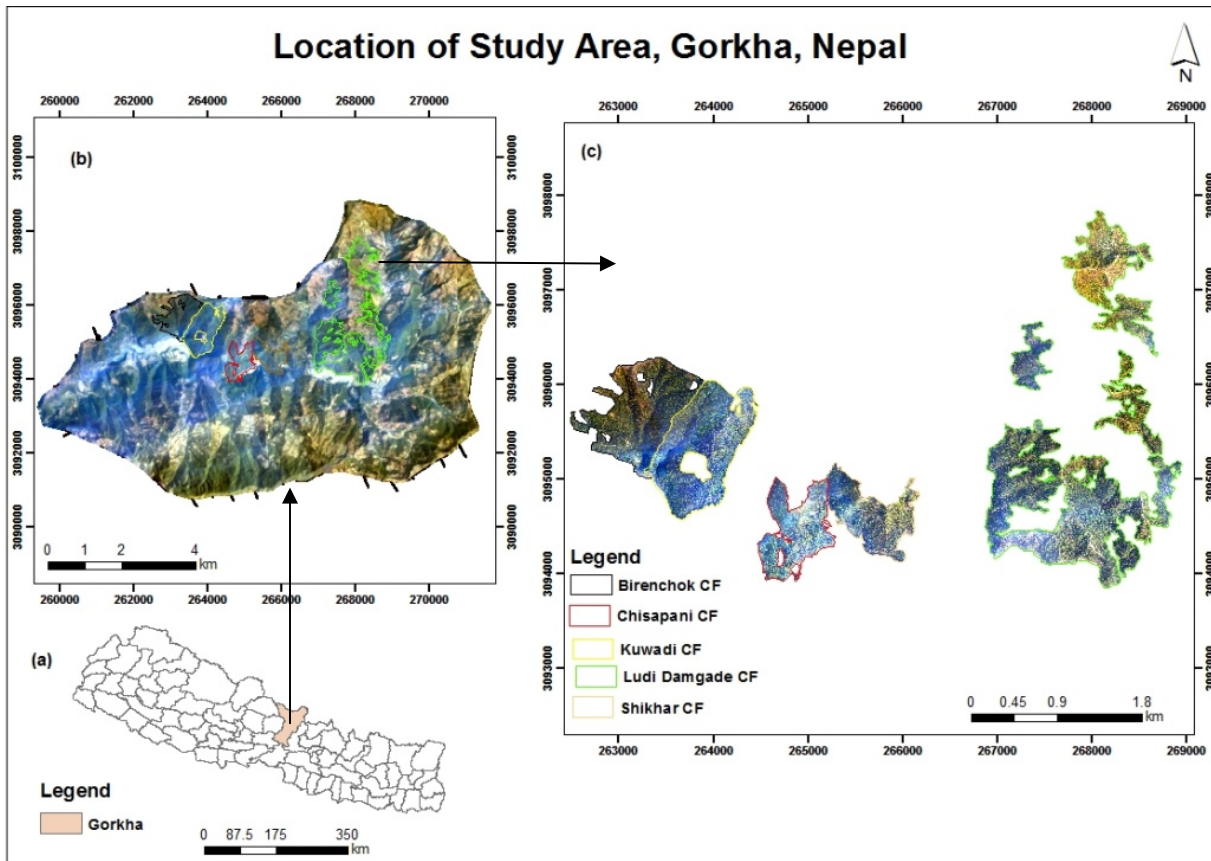


Figure 2.1: Study area, Gorkha, Nepal, (a) Nepal map (b) Ludikhola watershed (c) Selected CFs for the study

2.2.1. Socio-economic information and demography

The total population of the watershed is 23,197 with 3800 households comprising social diversity (ICIMOD et al., 2010). Ethnic groups such as Magar, Gurung, Tamang, Dalit, few Brahmin and Chhetri are prevailed in the watershed area. Agriculture is the main occupation of the area. About 70% of the total population is involved in subsistence agriculture (DSCO, 2006). Intergrated systems of farming, livestock and forest are being practiced in the area.

2.2.2. Topography

Ludikhola watershed lies in the mid-hill region of Nepal. The elevation of the watershed ranges from 318 m to 1714 m a.m.s.l. (ICIMOD et al., 2010). The terrain exhibits moderate to steep slope (30-60% slope) and also gentle sloping lands (less than 30% slope) are found.

2.2.3. Climate

With the altitudinal variation, the climate of the area varies. At lower altitude sub-tropical type of climate is found and at higher altitude, the climate is temperate. Summer, monsoon, autumn and winter are the main season in the area.

2.2.4. Temperature

An average daily temperature of Ludikhola watershed is 23.1°C (ICIMOD et al., 2010). The temperature has changed considerably in the past few decades and is increasing in a dramatic way (Lamichhane et al.,

2009). In 1978-1982, the average temperature recorded was 21.6°C and in 2001-2006 it was 23.1°C. Average monthly temperature of 1978 and 2006 is given in Appendix 1.

2.2.5. Rainfall

The average annual rainfall of the area is 1,972 to 2000 mm which occurs during Monsoon (July to September). There is gradual decrease in rainfall from 1980 to 1986 (1424.2 mm to 805.34 mm) and then gradual increase up to 1991 (1755.2 mm) (Lamichhane et al., 2009). Rainfall trend from 1978-2006 is given in Appendix 1.

2.2.6. Vegetation

The forest found in the area is subtropical type (Appendix 11). *Shorea robusta* is the dominant species of the forest in southern aspects and lower altitudes of northern aspects. In the upper parts of northern aspects *Schima wallichii* and *Castanopsis indica* are mainly found. List of tree species found in the study area is given in Appendix 2.

3. MATERIALS AND METHODS

3.1. Data Used

3.1.1. Digital Camera Imagery

Digital Camera imagery was used in the study. The imagery was acquired in March 2011. The image consists of 3 bands (red, green, blue) and has a resolution of 0.45 m. The image obtained for the study was already geo-referenced in UTM 45 N and orthorectified. Detailed specifications are given in Appendix 3.

3.1.2. LIDAR data

The LIDAR data was acquired for the purpose of national forest inventory of Nepal by FRA (Forest Resource Assessment) project under the Ministry of Forests and Soil Conservation. The data was collected from 16 March to 2 April 2011. The data was acquired by Arbonaut Ltd., Finland and it was already pre-processed by the company. The LIDAR data had point density of 0.8 point/m² on average. A detail of the LIDAR data acquisition is given in Appendix 4. The given LIDAR data was in the form of point cloud.

3.1.3. Maps

Topographic maps were used in the field data collection. Maps were at the scale of 1:25000 prepared by Survey Department of Government of Nepal. The watershed boundary of the study area, community forest and road shape files were obtained from ICIMOD in 2009.

3.1.4. Software

Various software as shown in Table 3.1 was used in this research.

Table 3.1: Softwares used in the research

S.N	Software	Purpose
1	ArcGIS version 10	GIS analysis
2	Erdas Imagine 2011	Image analysis
3	Lastools	Develop CHM
4	ecognition Developer 8	Object based image classification
5	R	Statistical analysis
6	Mirosoft Word	Thesis writing
7	Mirosoft Excel	Statistical analysis
8	MirosoftPowerpoint	Presentation of the research
9	Mirosoft Visio	Diagrammatic representation
10	End note	Citation and reference
11	Quick Terrain Modeler and Quick Terrain Reader	3D view of point cloud

3.1.5. Field Equipment

Various field equipment as shown in Table 3.2 was used during fieldwork.

Table 3:2: List of equipments used for the field work

S.N	Equipment	Purpose
1	iPAQ and Garmin GPS 60CSx	navigation
2	Suunto compass	orientation
3	Diameter tape 3meters	diameter measurement
4	Measuring tape 30 meters	measuring the radius of the plot
5	Spherical densiometer	crown cover measurement
6	Suunto clinometer	slope correction
7	Vertex hypsometer	tree height measurement
8	Fieldwork datasheet	field data record

3.2. Image pre-processing

Image pre-processing is also known as image restoration and rectification which increase the accuracy and interpretability of the data (Lillesand et al., 2008). Further manipulation and analysis of image data needs to be done to extract information. The obtained Digital Camera imagery was already georeferenced and orthorectified. Thus, georeferencing and orthorectification were not done. The obtained image was already mosaic by Arbonaut Limited. A subset of the image was created to extract the study area.

3.2.1. Image filtering

Image filtering is an image enhancement technique that is carried out for improving image interpretability. The image is smoothened when the average of pixel values in a given window size is calculated and that average value is used as the new value of the central pixel in the window (TTC, 2010). This is done for each pixel value. Window size of 3×3 , 5×5 and 7×7 are commonly used for individual tree crown delineation (Leckie et al., 2005; Mora et al., 2010; Tsendbazar, 2011). In this study, 3×3 low pass filter was used to smoothen the appearance of the image. This helped in manually delineating the tree crowns on the image.

3.3. Research Method

The research method followed three major steps i.e. data collection and preparation, remote sensing operations, and statistical analysis. Field work was carried out to collect the data about DBH, height and other measures whereas remote sensing operations were done to get the individual tree crown and height of each tree of the study area. Finally, statistical analysis was done to find the relationship between height, CPA and carbon for estimation and mapping carbon stocks. Methods to carry out this research are shown in Figure 3.1. Detailed description of each step is given in the following subsections.

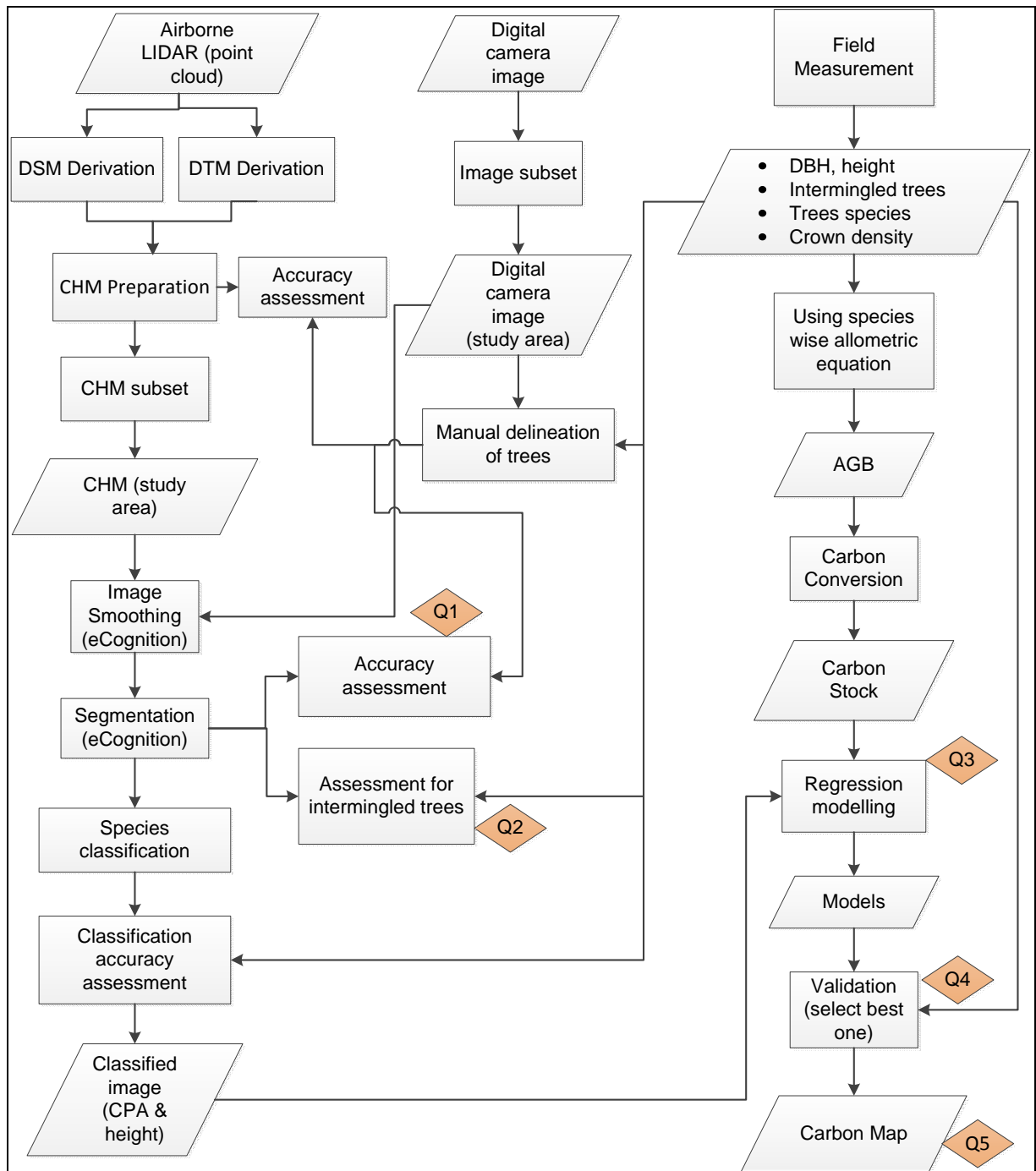


Figure 3.1: Flowchart of research method

3.3.1. Field work

Sampling design

An appropriate sampling design that covers both forest type and condition is essential. This is a critical step for improving estimation of carbon stocks (Gibbs et al., 2007). He recommended using a sampling design developed particularly for a specific country. Therefore, sampling design according to the

Community Forest Inventory Guideline of Nepal 2004 was adopted. Stratified random sampling helps to ensure that the sample is spread out over the entire study area and gives more precise estimates of the forest parameters (Husch et al., 2003). This sampling design gives less sampling error and coefficient of variation as it focuses at dividing population into a number of parts which are more or less homogenous for the specific parameters. Thus, stratified random sampling was applied for this research. Every community forest has its own characteristics in terms of altitude, age, slope, aspect and species composition. Stratification was done on the basis of these characteristics so that each community forest was taken as one stratum. The number of plots for the sampling was determined using following formula;

$$\text{Area of sampling (a)} = \text{sampling intensity (I)} \times \text{total area of stratum (A)} / 100 \quad (\text{DOF, 2004})$$

$$\text{No. of plot (n)} = \text{area of sampling (a)} / \text{area of one sample plot (p)}$$

The study area consisted of five CFs and each CF was considered as one stratum. The number of plots per stratum is shown in Table 3.3.

Table 3:3: Plot number in each stratum for data collection

S.N	Stratum	Plot number
1	Birechok CF	12
2	Kuwadi CF	10
3	Chisapani CF	10
4	Shikhar CF	8
5	Ludidamgade CF	46
Total		86

In order to identify the individual tree on the map in the field, enlarged maps (Appendix-5) for each plot with surrounding area were printed before field work.

Field data collection

Preparation such as field equipments collection, datasheet preparation (Appendix-6) and uploading image in iPAQ was done before the field work. The field work was carried out in September-October 2011. Circular plots with radius 12.62 m and plot area of 500 m² (IPCC, 2003) were used. Forest parameters such as DBH, height, crown diameter, crown density and species were recorded in the field. Intermingled trees were also recorded in each plot. If a tree crown was not visible as standalone i.e. completely separated from other crowns surrounding it, it was considered as intermingled even though their branches do not considerably intermixed together. Trees that were measured were marked to prevent double counting. Trees were measured from inward to the edge of the plot starting from North in clockwise direction. Besides these, information about topography such as slope and aspect were collected. Since trees with diameter 10 cm or less contribute little to the total carbon of the forest (Brown, 2002), only trees with diameter more of than 10 cm were taken into consideration for measurement. Slope correction was done in the sloping sample plot using slope correction factor Appendix 7. Trees on the image were recognized for each plot and were recorded. GPS and iPAQ were used for navigation to the plot centre. Tree parameters were measured in 86 plots. A map showing the total number of sample plots for data collection in the study area is given in Appendix-8.

3.3.2. Fieldwork data analysis

After completing field work, the data collected was entered in excel and descriptive analysis of the field data was done. Box plots were made for depiction of collected field data for major tree species. Identified trees on the image during the fieldwork were delineated using ArcGIS. The identified trees were used for species classification and its accuracy assessment. In addition, identified trees were used for developing and validation of the regression models.

3.3.3. Manual delineation of trees

The identified trees on the field were manually delineated on 3*3 low pass filtered image. Same scale (1:250) of the image was used while delineating all the trees. In order to delineate the trees correctly, crown diameter measured in the field was used as reference. Only 294 trees were recognized on the Digital Camera image and were manually delineated. These delineated tree crown areas were used to extract the height of the trees from the CHM and also used for segmentation accuracy assessment.

3.3.4. CHM (Canopy Height Model) Preparation

Canopy Height Model (CHM) is obtained by subtracting Digital Terrain Model (DTM) from Digital Surface Model (DSM) which gives the height of the trees (Kim et al., 2010). DTM represents bare ground surface whereas DSM represents ground surface including all objects on it (Heritage et al., 2009). DSM is generated from the first canopy return of the LIDAR pulse which describes the canopy surface and DTM is generated from the last returns which describes ground surface.

The given LIDAR data was in the form of point cloud. From the point cloud, DTM and DSM were developed using Lastools software. This software has the tools required to develop DTM and DSM from raw or pre-processed LIDAR data (point clouds) (Hug et al., 2004) and this is free software. DSM was created using only first returns using the Lasgrid tool. Then, cell size of 0.45 m was used as the LIDAR data was to be merged with Digital Camera image which has the cell size of 0.45 m. The highest elevation value was chosen from all points falling into a grid cell for raster generation.

To create DTM, Lasground tool was used to classify point clouds into ground points and non-ground points. Then, DTM was developed by blast2dem tool using only ground points. The same cell size was given. This tool creates a raster DTM in which elevation values of a raster cell is assigned based on TIN (Triangulated Irregular Networks) interpolation.

After creating DTM and DSM, CHM was developed by subtracting DTM from DSM. The obtained CHM was then filtered as there was noise resulting in high variation in height values of trees which are not true in reality. The maximum height measured in the field was 35.3 m. Based on this information, CHM was filtered and height up to 40 m was taken.

3.3.5. Accuracy assessment of LIDAR derived height

Accuracy assessment of LIDAR derived height was done by comparing height of the trees measured in the field and height of the trees obtained from the CHM (Hyypä et al., 2000; Suárez et al., 2005). In the field, tree tops were measured for trees height. These trees which were recognized on the image were manually delineated. For the same trees, maximum height values from the CHM were extracted using manually delineated crowns because they represent the tree tops. Then, coefficient of determination (R^2) was obtained for the tree height from the field and from the CHM. Further, RMSE was calculated. Then, average field measured height was also compared with the average LIDAR derived height.

3.3.6. Tree crown delineation

Tree crown delineation (segmentation) is an initial step of object based image analysis which involves grouping neighbouring pixels into meaningful image objects (segments) based on homogeneity criteria. There are several ways to segment an image. Most appropriate method should be chosen for a particular image analysis. In this study, chessboard segmentation and region growing approach were used in eCognition software to derive the image objects or tree crowns. Both Digital Camera image (3 bands, RGB) and CHM (1 band) were used for image segmentation in eCognition software. The image segmentation process was as follows;

Pre-processing in eCognition

Both the Digital Camera image and the CHM were pre-processed in eCognition. CHM was smoothen to avoid the finding of false tree tops within a tree (Reitberger et al., 2007) and Digital Camera image was filtered to remove noise and smoothen the image (ITC, 2010). This was done by applying a Convolution filter to both images. Convolution filter replaces each pixel value by the average of the square of the matrix centred on the pixel (eCognition, 2011a). For this, 3×3 kernel size was used for the filtering.

Chessboard segmentation

Chessboard segmentation is top-down segmentation in which an image is split into smaller image objects into equal squares of a given size (Figure 3.2) which are in subsequent processes aggregated into meaningful objects. Square grids of fixed size are applied to all objects in the domain and each object is cut along these grid lines (Definiens, 2007). Grid size of two by two pixels was used for chessboard segmentation considering the processing capability of eCognition.

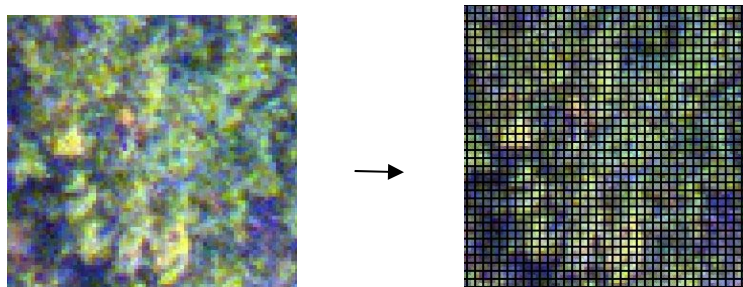


Figure 3.2: Chessboard segmentation

After chessboard segmentation, the resulting objects were split into two preliminary classes: tree and others. For the assigning of pixels to classes, information from both CHM and Digital Camera image were used. The mean brightness values from the image and height information from CHM were used to assign the classes. Objects (trees) with height of less than 2 m were removed (Naesset, 1997) and only those of more than 2 m are taken for segmentation because the shrubs were found up to 2 m height in the study area and the study is on carbon stocks estimation of the trees only. In addition, during field study lopped trees with no crowns were found up to the 2 m height. Thus, for segmentation it is necessary to remove such lopped trees which had no crowns. Besides, their contribution to the carbon stock is minimal since they are relatively small.

Region Growing approach

In this approach, regions are grown from the seed points based on certain rules. The pixels neighbouring a seed point are then joined to this region and the process is continued until it reached the threshold (Blaschke et al., 2006). To run this algorithm for the delineation of tree crowns, firstly it is necessary to

identify the seed points and define the threshold to stop the region growing. Culvenor (2002) stated that local maxima (peaks) and local minima (valleys) are the fundamental image features used for the delineation of tree crowns. Local maxima are used as seed points to grow into meaningful objects and local minima are used to define likely crown boundaries (Culvenor, 2002). The algorithm assumes that the centre of the crown is brighter than the edges (Culvenor, 2002). Local maxima are thus tree tops which looks like peak of the mountain and local minima looks like valley which is shown in Figure 3.3.

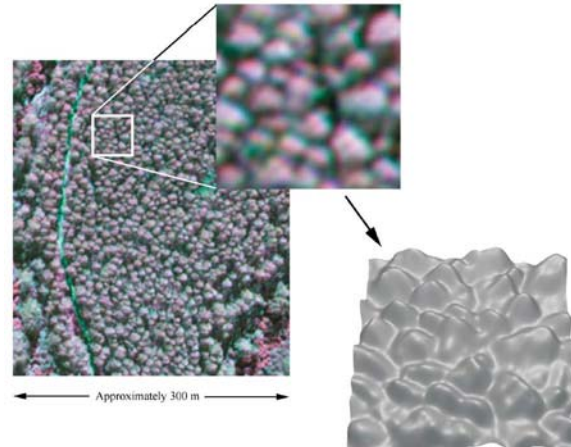


Figure 3.3: Radiometric 'topography' of subset of VHR image of forest, source: (Culvenor, 2002)

In this study, tree crown delineation was done based on growing of tree tops using local maxima and local minima to define likely crown boundaries. Appropriate window size or threshold should be chosen in this method because treetop detection can vary with window size. If the window is small, for the tree with large crown may detect more than one tree top and if the window size is bigger, then it may not be able to detect tree tops for smaller trees. In this case, window size of 5×5 was taken as average crown diameter measured in the field was approximately 4 m.

Firstly local minima were identified and local minima which were too close to each other were merged because this may create confusion in the segmentation. They will form the edge of the segmented object or the boundary of the tree crown. Then, tree tops (local maxima) were identified. However, all identified tree tops were not true tree tops because the algorithm identified more than one tree top for a single tree. A tree may have several tops on a fairly flat upper canopy and in such condition false tree tops are detected. To remove false tree tops, at first tree tops were grown and then grown tree tops which neighbour to one another were merged. Then, region growing from the tree tops was done until it reached the local minima. Tree crowns were grown in relation with neighbouring objects. Then, basic reshaping of tree crown segments was done. This was done by removing small objects (object area ≤ 4 pixels) and asymmetrical crown segments. Local maxima and local minima were identified using height information from CHM and for the region growing, information from both the images were used.

Advanced reshaping of tree crown segments

After basic reshaping of tree crown segments, watershed transformation and morphology was done. These are advanced object reshaping algorithms (eCognition, 2011a). Watershed transformation was used to split the obtained crown segments which may consists of several trees close together into individual tree crown segment. This algorithm helps to separate cluster of trees into individual trees. The basic concept of watershed transformation is based on visualizing the image to be processed as topographic surface and includes three basic notions: local maxima, catchment basins and watershed lines (Chen et al., 2006). The image is inverted due to which local maxima become local minima and holes are punched at

the local minima. Catchment basins are in between local maxima and local minima. When water is introduced from the local minima, catchment basins will be flooded and barriers need to be created to prevent merging of water coming from two neighbouring catchment basins. These barriers are the watershed lines and will be used to partition trees. Thus, when watershed transformation is applied to the forest, tree clumps are treated as catchment basins and watershed lines are their edges thus separating clusters of trees into individual trees.

Then, morphology algorithm was applied to smoothen the edges of tree crowns. After this, basic reshaping of tree crown segments was done again based on the object (crown segment) area and roundness. The overall segmentation process is given in Figure 3.4.

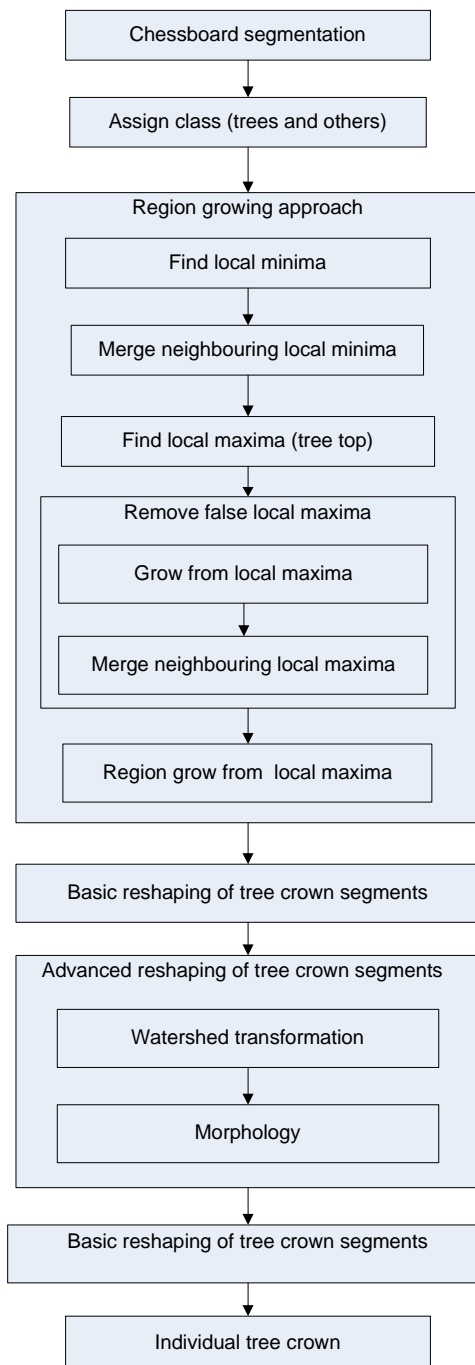


Figure 3.4: Steps for tree crown delineation

3.3.7. Accuracy assessment of tree crown delineation

Accuracy assessment of tree crown delineation is related to the matching of reference and automatic segmented objects (Zhan et al., 2005). Reference objects means manually delineated polygons. There are several methods for segmentation validation (Zhang, 1996). However, in this study two segmentation accuracy measures were applied i.e. Relative Area measures developed by Clinton et al. (2010) and 1:1 correspondence (Zhan et al., 2005). These measures are applied when manually delineated and automatic segments are available.

Clinton et al. (2010) reviewed several segmentation accuracy measures and modified Relative Area measures developed by Moller et al. (2007). Over segmentation and under segmentation defined by Clinton et al. (2010) are given in equation 1 and 2.

$$\text{Over segmentation}_{ij} = 1 - \frac{\text{area}(x_i \cap y_j)}{\text{area}(x_i)} \dots\dots\dots 1$$

$$\text{Under segmentation}_{ij} = 1 - \frac{\text{area}(x_i \cap y_j)}{\text{area}(y_j)} \dots\dots\dots 2$$

Where x_i is the reference object and y_j is the corresponding segmented object.

The value of over segmentation and under segmentation lies within the range of 0 to 1 (Clinton et al., 2010). When the value for both over and under segmentation is 0, then it is considered as perfect segmentation. It means segments matched exactly with the reference objects. Using over segmentation and under segmentation values, segmentation goodness (D) can be calculated. D (equation 3) is interpreted as the ‘closeness’ to an ideal segmentation result, in relation to a predefined reference objects (Clinton et al., 2010). D value ranges from 0 to 1. D value equals to 0 means perfect segmentation.

$$D = \sqrt{\frac{\text{over segmentation}^2 + \text{under segmentation}^2}{2}} \dots\dots\dots 3$$

1:1 correspondence was done by matching manually delineated tree crowns with automated segments. Matching was considered if manually delineated and automatic segments overlap by at least 50% (Zhan et al., 2005). There are several possibilities of two matched polygons which are shown in Figure 3.5. All the possibilities shown in Figure 3.5 are considered as matching by the above criteria.

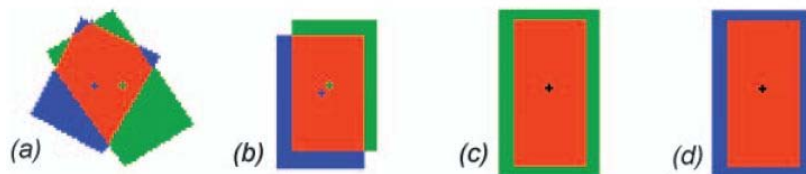


Figure 3.5: Different conditions of 1:1 correspondence, source: (Zhan et al., 2005)

Red region in Figure 3.5 shows the matched regions whereas green is the region that is not explained by reference object. Blue is the region of reference object which is not overlapped. Example (a) shows more than 50% match between reference and segment object; (b) shows matching reference and segmented objects with the same shape and size but differ in position; (c) and (d) matching reference and segment objects with the same position but differ in spatial extent.

3.3.8. Segmentation assessment for intermingled trees

In order to assess whether intermingled trees are separated or not using LIDAR data, segmentations were checked based on visual interpretation. From the field data, it is known that where those intermingled trees are in each plot. Then, segmentation was checked visually for each identified intermingled trees on the image. If there are two segments for two trees which appeared to be intermingled in the field, then intermingled trees are considered separated.

3.3.9. Image classification

Object based image classification is particularly suitable for VHR images and data obtained by airborne laser scanning (ALS) or microwave radar (ITC, 2010). In addition to the spectral information, this method use shape, texture and contextual information to interpret the image. There are two types of classification method available in eCognition i.e. membership function and nearest neighbour.

Nearest neighbour classification was applied for tree species classification. It was applied to selected object features and was trained by the samples. Here the samples are the image objects (segments) obtained from the segmentation. After training the software using the samples, image objects will be classified based on their nearest sample neighbours (eCognition, 2011b).

Although *Shorea robusta*, *Schima wallichii*, *Castanopsis indica* and *Rhus wallichii* are the dominant tree species in the study area, classification was done only into two classes i.e. *Shorea robusta* and others. This is because most of the trees identified on the image were *Shorea robusta* and there were not enough *Schima wallichii*, *Castanopsis indica* and *Rhus wallichii* identified on the image. Thus, there were an insufficient number of samples of these species to train the image objects for classification and also for the validation. 70% of the data were used for training classification and 30% of the data was used for accuracy assessment.

3.3.10. Classification accuracy assessment

The output of the image classification is a raster file in which the individual raster elements are class labelled (ITC, 2010). It is necessary to check the actual quality of the classification result. It is done by selecting a number of objects of the classification output and compare the classification result and the true world classes i.e. field observations (ITC, 2010). Comparison is done using error matrix from which various accuracy measures can be computed. Classification accuracy assessment was done in Erdas Imagine 2011.

3.3.11. Above Ground Biomass and Carbon Stock calculation

Site specific allometric equations were not available for the tree species found in the study area. Thus, the allometric equation developed for tropical moist forest by Chave et al. (2005) was used to calculate AGB. The equation was also applied by REDD+ pilot project (ICIMOD et al., 2010). The equation is given below;

$$AGB = 0.0509 \times \rho D^2 H \quad \dots\dots\dots 4$$

Where,

- AGB = above ground biomass [kg]
- ρ = wood specific gravity [gm/cm³]
- D = tree diameter at breast height (DBH) [cm] and
- H = tree height [m]

Trees found in the study area were classified into two; namely *Shorea robusta* and others. Wood specific gravity for *Shorea robusta* is 0.88 gm/cm³ and for others is 0.72 gm/cm³ (ICIMOD et al., 2010). Then carbon stock of the tree was calculated from AGB using conversion factor 0.47 (IPCC, 2003).

$$\text{Carbon stock} = 0.47 \times \text{AGB} \quad \dots\dots\dots 5$$

3.3.12. Regression analysis and model validation

Regression analysis is frequently used for AGB estimation. Regression analysis is carried out for determining the relationship between response variable and one or more explanatory variables. The analysis quantify the relationship and is expressed by an equation and its graphic representation (Husch et al., 2003). There are two methods commonly used to evaluate the model performances i.e. coefficient of determination (R²) and root mean squared error (RMSE). Generally high R² or low RMSE value show a good fit between observed and predicted outcomes (Lu, 2006). R² shows how much a model can explain the reality. RMSE is one of error indices commonly used for model evaluation. It shows error in unit of the constituent of the interest. In this study, RMSE gives error in kg. RMSE is calculated as follows;

$$\text{RMSE} = \sqrt{\frac{1}{n} \sum_{i=1}^n (X_{O_i} - X_{P_i})^2} \quad \dots\dots\dots 6$$

Where,

X_O = Observed carbon

X_P = Predicted carbon

n = Number of observations

Then, RMSE in percentage was calculated from the ratio of RMSE and average observed carbon.

Three regression models were developed based on the linear relationships between carbon and CPA, carbon and height and carbon, CPA and height. Before developing the relationship of carbon with CPA and height, multicollinearity was checked for two independent variables i.e. CPA and height. Multicollinearity was detected by calculating the Variation inflation Factor (VIF). VIF value above 10 indicates that there will be effect of multicollinearity on the model (Obrien, 2007).

Only trees which had one to one matching of the segments and correctly classified were taken for model development and validation because incorrectly identified and misclassified trees should not be used for evaluation (Pouliot et al., 2002). Outliers were removed which is the prerequisite of the regression models (Mora et al., 2010). Therefore, total number of sample data becomes lesser than the trees that were initially identified on the image. Only 239 trees were used for model development and validation. For model development and validation, the data was divided into 70% and 30% respectively. Models were validated by comparing the amount of carbon calculated from the field data and carbon predicted by the model.

Same number of observations was used to develop the models so that the models can be compared. For *Shorea robusta* it was 132 and for others it was 47. The accuracy of developed models was compared based on RMSE.

3.3.13. Carbon stock mapping

Multiple linear regression models were used for both *Shorea robusta* and other species to estimate the amount of carbon stocks in the study area. These models were chosen as RMSE% was the lowest compared to other models. Then, a carbon map of the study area was produced using ArcGIS.

4. RESULTS

4.1. Descriptive analysis of the field data

A total number of trees inventoried were 2793 and about 294 trees from the field were recognized on the image. The data were collected in 86 sample plots from five CFs. Among five CFs, Ludidamgade was the largest CF so that this CF had largest number of sample plots. In this CF, 1534 trees were measured among which 186 trees were recognized. There were altogether 316 intermingled trees. A detail of forest inventory is shown in Table 4.1. Descriptive statistics of collected data is given in Appendix 9.

Table 4.1: Forest inventory

S.N	Name of CF	No. of plots	Total trees inventoried	Intermingled trees	Recognized trees on the image
1	Birenochok	12	451	72	41
2	Shikhar	8	129	17	17
3	Chisapani	10	269	21	20
4	Kuwadi	10	410	62	30
5	Ludidamgade	46	1534	144	186
Total		86	2793	316	294

There were 27 tree species found in the study area (Appendix 2). Among them, the dominant species was *Shorea robusta* followed by *Schima wallichii*, *Rhus wallichii*, *Castanopsis indica*, *Pinus roxburghii*, *Terminalia alata* and *Cleistocalyx operculata*. Beside these species, other species were categorized into one and given the name ‘Others’ as their occurrence was less than 1%. A detail of occurrence of the tree species recorded during the field study is given in Figure 4.1.

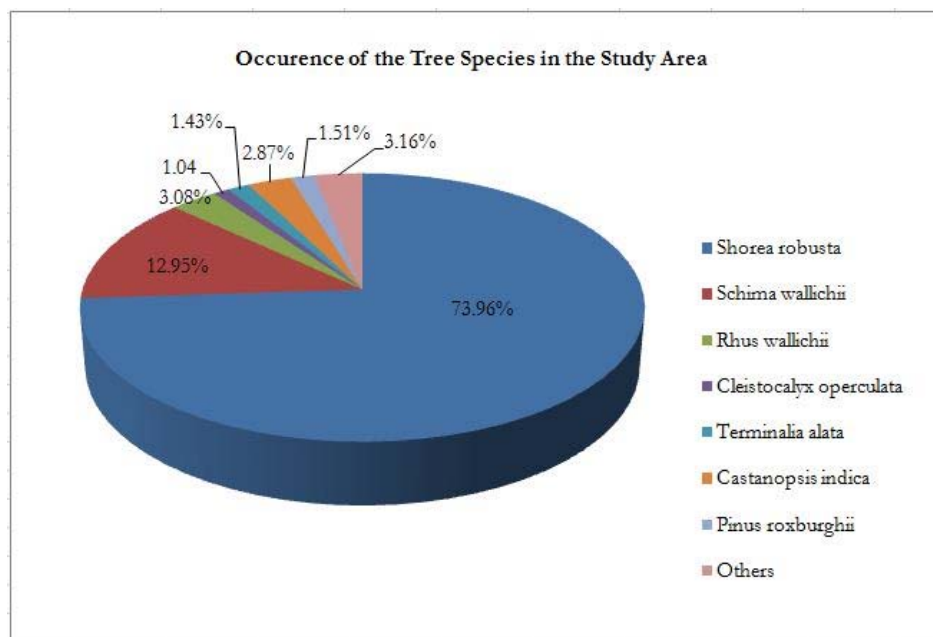


Figure 4.1: Tree species occurrence in the study area

DBH and height of major tree species (more than 2% occurrence) were analyzed and presented by box-plots which are given in Figure 4.2. *Schima wallichii* has the largest and *Castanopsis indica* has the smallest DBH on average. The mean height of the *Shorea robusta* is found to be the highest followed by *Castanopsis indica*, *Schima wallichii* and *Rhus wallichii*. For the both DBH and height, the highest variability is found in *Shorea robusta*. This was expected due to the high number of sample trees of this species. The least variability for DBH values is found in *Castanopsis indica* and for height values, it is found in *Rhus wallichii* but this is probably due to the low number of sample trees of the species.

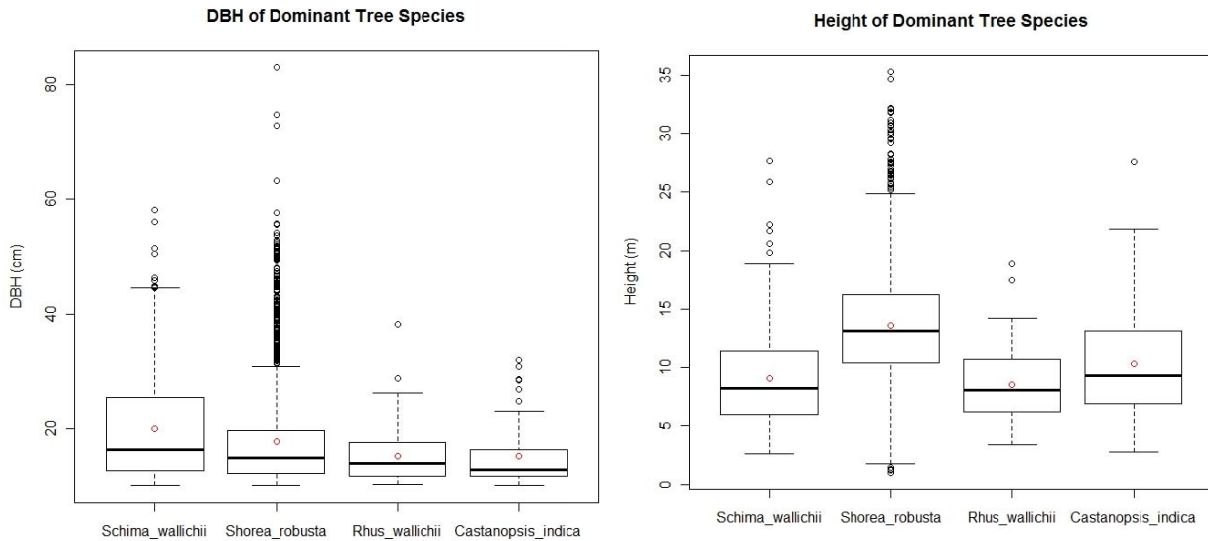


Figure 4.2: DBH and height of the major tree species

Groups of two intermingled trees were followed by groups of three and four intermingled trees (Figure 4.3). This was occurred mainly in *Shorea robusta* which was dominant tree species in the forest. A majority of trees were found intermingled within the same species and least was found with different species. Three and four intermingled trees were observed only in *Shorea robusta* with the same species. The total number of trees resulted in 274, 30, and 12 trees with two, three and four intermingled trees respectively.

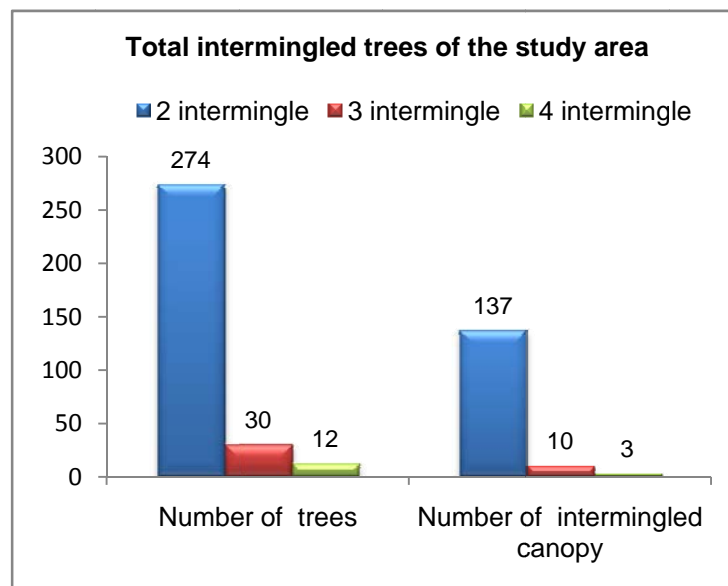


Figure 4.3: Number of intermingled trees

4.2. CHM preparation and accuracy assessment of LIDAR derived height

CHM developed by subtracting DTM (Figure 4.4 b) from DSM (Figure 4.4 a) is shown in Figure 4.5. Its value ranges from 0-40 m. Height of 0 m means there is no tree which is represented by black colour.

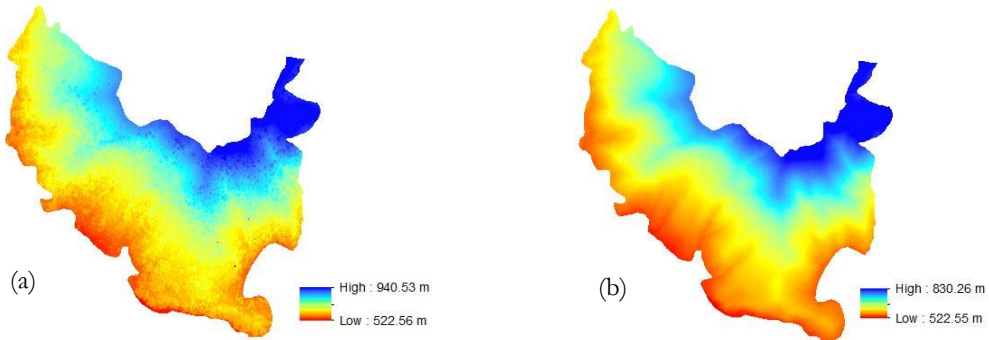


Figure 4.4: (a) DSM and (b) DTM derived from point cloud

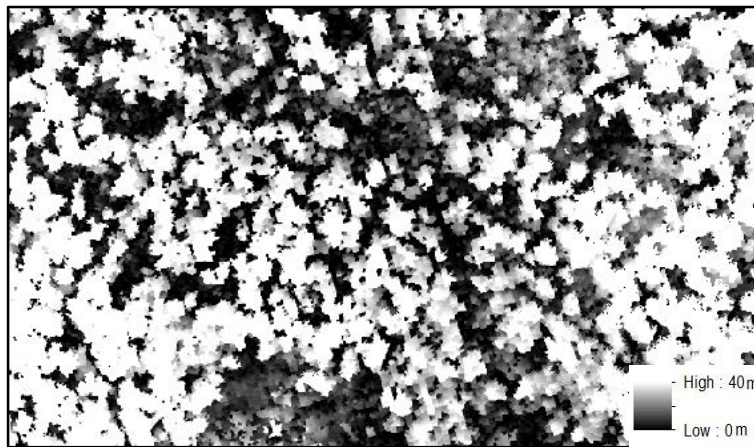


Figure 4.5: CHM of the study area

LIDAR derived height was compared with field measured height using linear regression model as shown in Figure 4.6. This was done using approximately 281 observations. Coefficient of determination (R^2) was 0.74 and RMSE of 2.8 m was obtained. There was an underestimate of field measured tree height by 0.98 m on average.

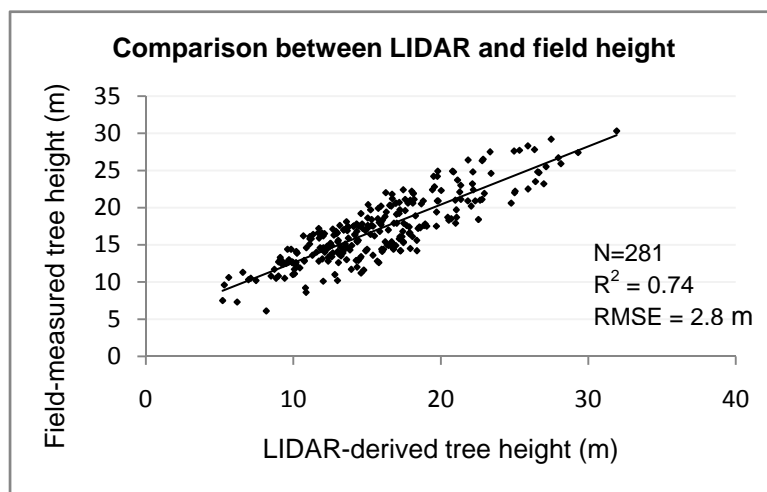


Figure 4.6: LIDAR derived tree height compared with field measured tree height

4.3. Tree crown delineation and accuracy assessment

Individual tree crown delineation was done using region growing approach. Figure 4.7 shows results of several steps to delineate individual tree crowns in Ludidamgade CF.

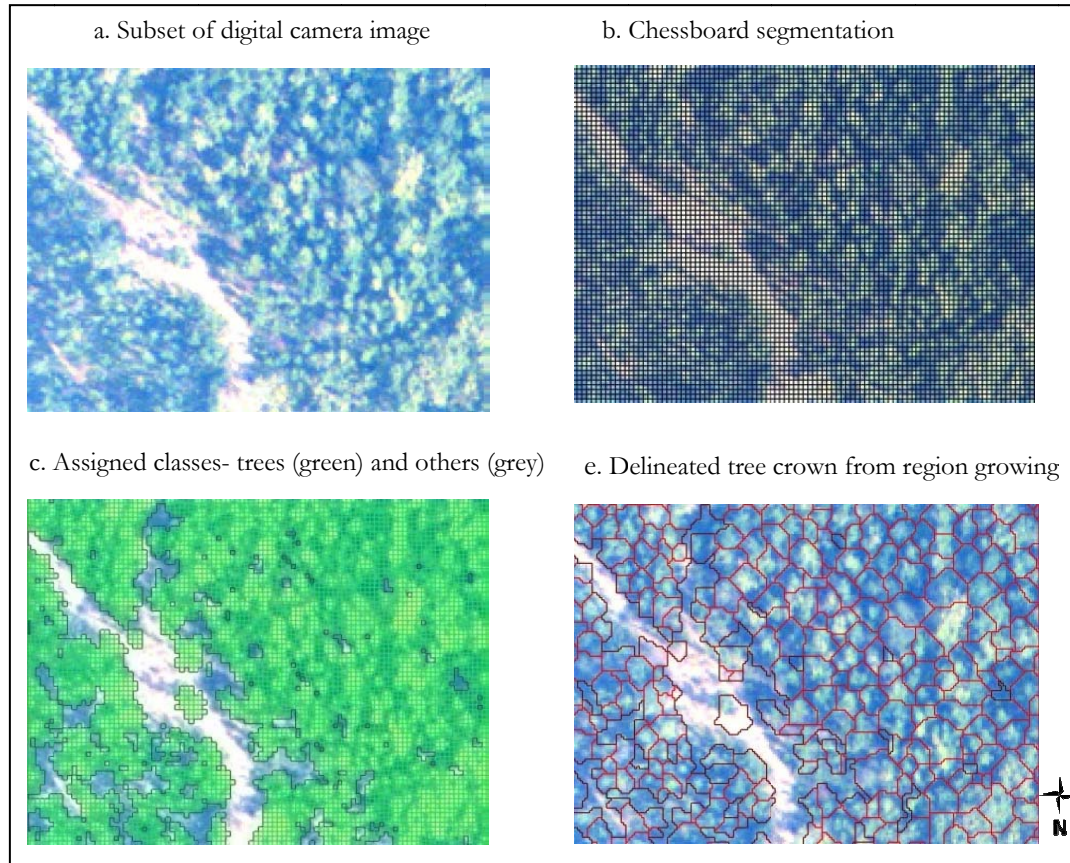


Figure 4.7: Tree crown delineation using region growing approach

Accuracy assessment of tree crown delineation was done using accuracy measures of D and 1:1 correspondence for 294 manually delineated tree crowns. For the all delineated tree crowns of the study area, over segmentation was 0.29, under segmentation was 0.33 and D value was 0.31. This means over segmentation error was 29%, under segmentation error was 33% and total tree crowns delineation had 31% error (69% accurate). For the accuracy measures of 1:1 correspondence, manually delineated tree crowns and automated segments from segmentation were assessed by matching on one to one basis. On the basis of this accuracy measures, overall segmentation accuracy was 76.2%. Out of 294 manually delineated reference tree crowns, 224 automated segments had one to one relationships. Thus, the first hypothesis mentioned in section 1.4 is not rejected as the accuracy of tree crown delineation is more than 70%. The result is shown in detail in Table 4.2.

Table 4.2: 1:1 Correspondence of reference and segmented CPA

CFs	Total reference CPA	Total number of 1:1 match	Correctly segmented CPAs in %
Birenochok	47	42	89.36
Kuwadi	49	43	87.76
Chisapani	19	12	63.16
Shikhar	17	11	64.71
Ludidamgade	162	116	71.6
Overall	294	224	76.2

4.4. Image classification and accuracy assessment

Image classification was done with nearest neighbourhood classification algorithm in eCognition. Trees were classified into two groups i.e. *Shorea robusta* and others. The classified map is given in Figure 4.8.

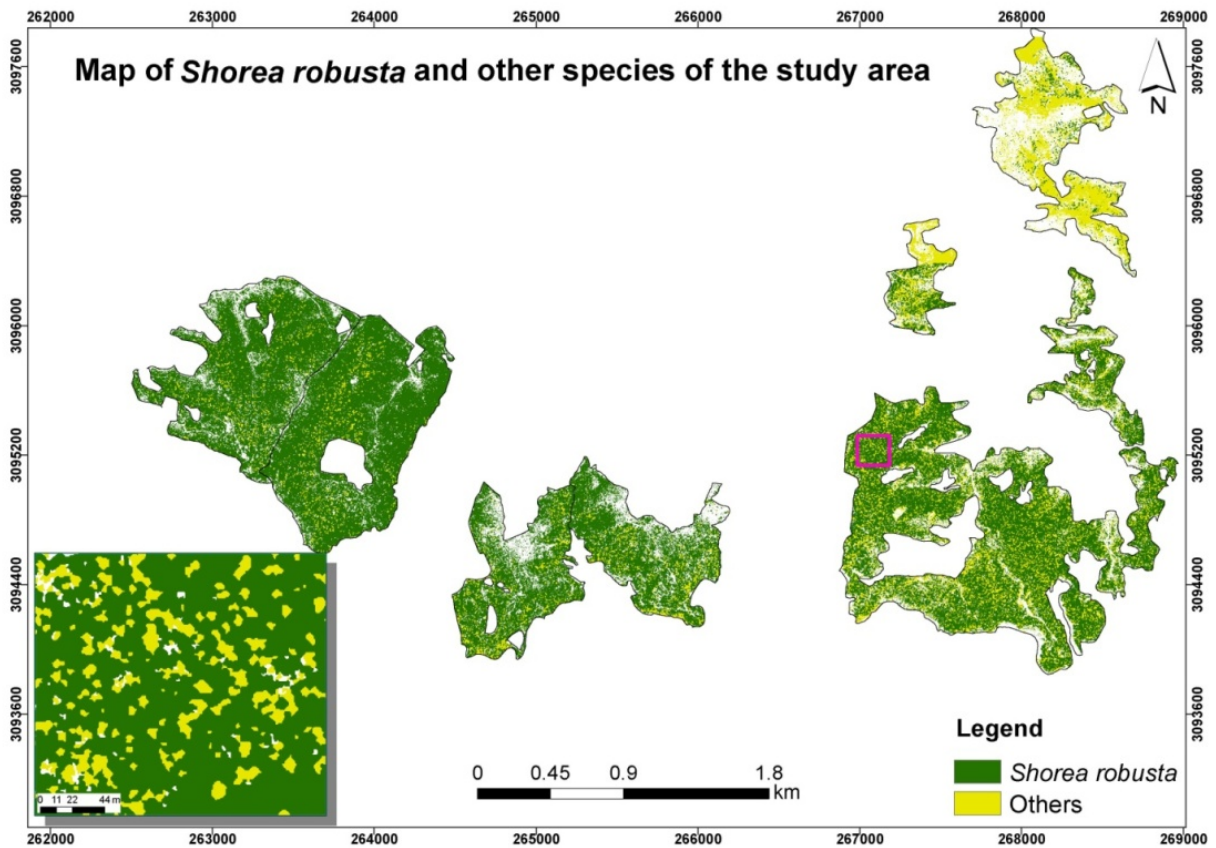


Figure 4.8: Tree species map of the study area in Ludikhola watershed, Gorkha, Nepal

Tree species classification was validated using 87 observations out of which 59 observations were for *Shorea robusta* and 28 observations were for other species. The classification was assessed based on overall classification accuracy, user accuracy and producer accuracy using error matrix shown in Table 4.3. For *Shorea robusta*, 54 observations (*Shorea robusta*) were correctly classified whereas 5 observations (*Shorea robusta*) were incorrectly classified as others. In case of other species, 12 observations (others) were correctly classified while 16 observations (others) were misclassified as *Shorea robusta*. Both producer

accuracy and user accuracy were higher for *Shorea robusta* than other species. The overall accuracy of the classification was 75.86%.

Table 4:3: Accuracy assessment of tree species classification

Class Name	Reference data		Classified Totals	Error of Commission (%)	User Accuracy (%)
	<i>Shorea robusta</i>	Others			
<i>Shorea robusta</i>	54	16	70	23	77
Others	5	12	17	29	71
Totals	59	28	87		
Error of Omission (%)	9	57			
Producer Accuracy (%)	91	43			
Overall Classification Accuracy = 75.86%					

4.5. LIDAR data in separating intermingled tree crowns

Out of 316 intermingled trees observed in the field, only 101 intermingled trees were recognized on the image. After segmentation, intermingled trees were checked whether the automated segment include only one tree or more than one tree. No intermingled trees were found to be separated. Figure 4.9 shows intermingled trees that were not separated.

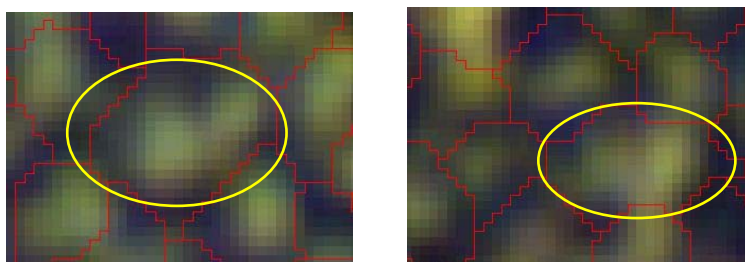


Figure 4.9: No separation of intermingled trees

4.6. Model development and validation

In this study, two variables, tree height and CPA were obtained using LIDAR data and Digital Camera image. Relationship between CPA and carbon; height and carbon; CPA, height and carbon were developed for *Shorea robusta* and other species. Results are described below.

4.6.1. Relationship between CPA and Carbon

Linear regression models (Table 4.4) were developed to derive the relationship between CPA and carbon for both *Shorea robusta* and other species. A total of 132 measurements were used for model development in case of *Shorea robusta* where as a total of 47 measurements were used in case of the other species. The coefficient of determination (R^2) for *Shorea robusta* and other species were 0.62 and 0.61 respectively (Figure 4.10). The regression analysis showed good correlation between CPA and carbon for both the classes with the correlation coefficient varying from 79% (*Shorea robusta*) to 78% (others). The models developed for carbon stock estimation of *Shorea robusta* and other species are;

$$\begin{aligned} \text{Carbon Stock}(\textit{Shorea robusta}) &= -8.99 + 11.72 \times \text{CPA} \dots\dots\dots 1 \\ \text{Carbon stock}(\textit{Others}) &= 2.19 + 7.68 \times \text{CPA} \dots\dots\dots 2 \end{aligned}$$

Table 4:4: Regression analysis of *Shorea robusta* and other species

	Coefficients	Standard Error	t Stat	P-value	Species
Intercept	-8.99	16.71	-0.54	0.59	<i>Shorea robusta</i>
Slope (CPA)	11.72	0.81	14.56	4.48E-29	
Intercept	2.19	18.52	0.12	0.91	others
Slope (CPA)	7.68	0.92	8.38	9.8E-11	

One way Analysis of Variance (ANOVA) test at 95% confidence level (Appendix 10) showed the significant relationship between carbon and CPA.

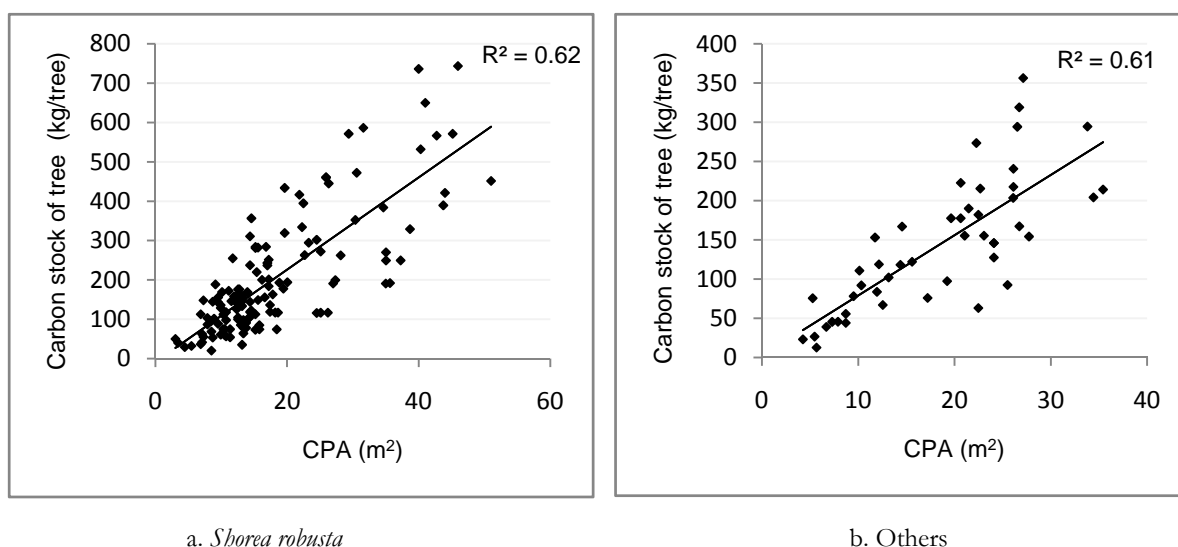


Figure 4.10: Relationship between CPA and carbon

4.6.2. Relationship between height and Carbon

Linear regression models (Table 4.5) were developed to derive the relationship between height and carbon for both *Shorea robusta* and other species. A total of 132 measurements were used for model development in case of *Shorea robusta* where as a total of 47 measurements were used in case of the other species. The coefficient of determination (R²) for *Shorea robusta* and other species were 0.64 and 0.63 respectively (Figure 4.11). The regression analysis showed good correlation between height and carbon for both the species with the correlation coefficient varying from 80% (*Shorea robusta*) to 79.4% (others). One way ANOVA test at 95% confidence level (Appendix 10) showed the significant relationship between height and carbon. The models developed for carbon stock estimation of *Shorea robusta* and other species are;

$$\text{Carbon stock (Shorea robusta)} = -241.41 + 28.97 \times \text{height} \dots\dots\dots 3$$

$$\text{Carbon stock (Others)} = -58.48 + 14.98 \times \text{height} \dots\dots\dots 4$$

Table 4:5: Regression analysis of *Shorea robusta* and other species

	Coefficients	Standard Error	t Stat	P-value	Species
Intercept	-241.41	32.79	-7.36	1.84E-11	<i>Shorea robusta</i>
slope (Height)	28.97	1.91	15.14	1.78E-30	
Intercept	-58.48	26.48	-2.21	0.03	others
Slope (Height)	14.98	1.72	8.69	3.46E-11	

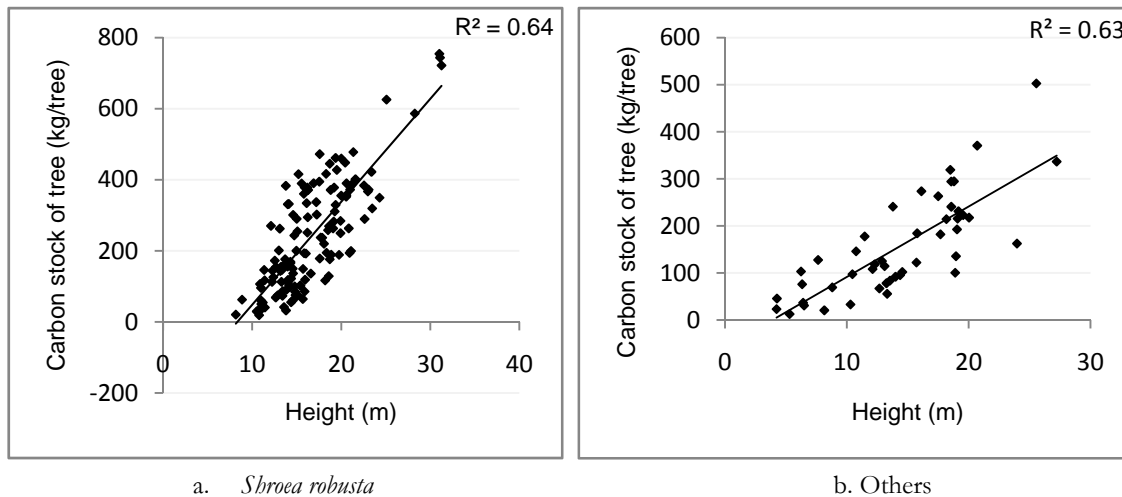


Figure 4.11: Relationship between height and carbon

4.6.3. Relationship of Carbon with CPA and height

In order to derive the relationship of carbon with CPA and height, firstly the multicollinearity was tested. This was done by checking the correlation between CPA and height for both *Shorea robusta* and other species. The correlation coefficient for *Shorea robusta* was 0.58 and Variance inflation factor (VIF) was 1.51 whereas for other species correlation coefficient was 0.34 and VIF was 1.13. This indicates that there will not be effect of multicollinearity on the model.

Multiple linear regression models (Table 4.6) were developed for both *Shorea robusta* and other species. For the models, a total of 132 observations were used for *Shorea robusta* whereas that for other species was 47. R² for *Shorea robusta* and other species were 0.72 and 0.67 respectively while adjusted R² for *Shorea robusta* was 0.72 and for other species it was 0.65. One way ANOVA test at 95% confidence level showed the models were significant (Appendix 10). The model developed for carbon stock estimation for *Shorea robusta* and other are;

$$\begin{aligned} \text{Carbon stock (Shorea robusta)} &= -163.07 + 10.58 \times \text{CPA} + 11.58 \times \text{height} \dots\dots\dots 5 \\ \text{Carbon stock (Others)} &= -102.2 + 6.2 \times \text{CPA} + 9.48 \times \text{height} \dots\dots\dots 6 \end{aligned}$$

Table 4:6: Multiple linear regression using height, CPA and carbon

	Coefficients	Standard Error	t Stat	P-value	Species
Intercept	-163.07	38.87	-4.20	5.02E-05	<i>Shorea robusta</i>
slope (CPA)	10.58	0.73	14.50	7.15E-29	
slope (height)	11.58	2.46	4.71	6.42E-06	
Intercept	-102.2	33.51	-3.05	0.003	others
slope (CPA)	6.2	0.92	6.78	2.47E-08	
slope (height)	9.48	2.32	4.08	0.0001	

4.6.4. Model validation

Models thus developed were validated against the field observed datasets (n=35, *Shorea robusta*; n=25, others). The results of the modelling corresponded well with the observed values (Figure 4.12).

In general, all models were explaining the relationship of carbon with CPA and height. Comparing all models, multiple linear regression models had the lowest RMSE% i.e. 36.8% and 32.4% for both *Shorea robusta* and other species respectively. This means there is 36.8% average error in the prediction of carbon for *Shorea robusta* and 32.4% average error in the prediction of carbon for other species. The relationship between CPA and carbon for both classes of trees resulted in higher RMSE% i.e. 47.1% for *Shorea robusta* and 41.5% for other species. RMSE% of the model developed for height and carbon were 40.3% and 35.3% for *Shorea robusta* and other species respectively. The last hypothesis mentioned in section 1.4 is not rejected because multiple regression models have the lowest RMSE% compared to other models. This means multiple regression models improve accuracy of carbon estimation than other models.

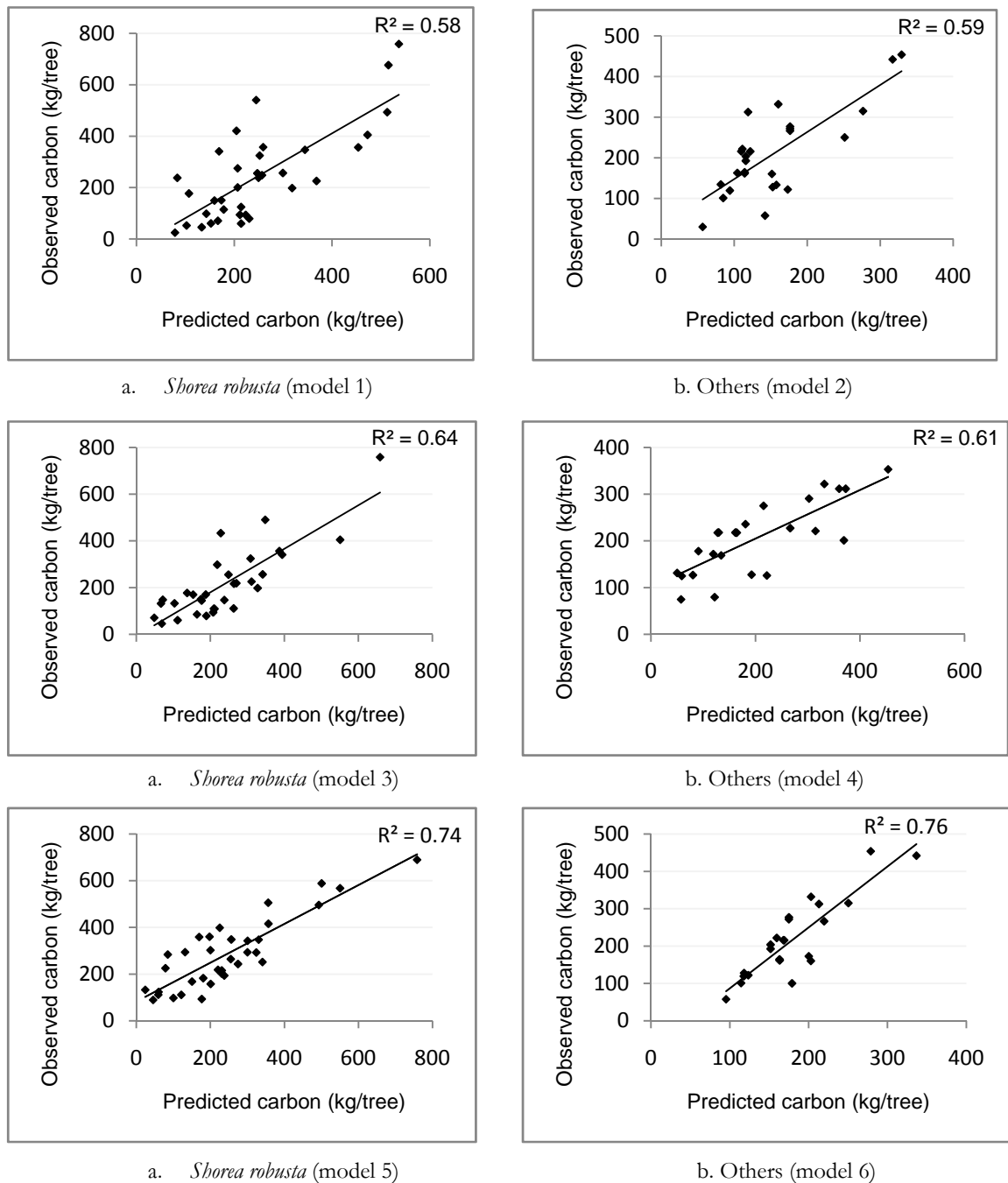


Figure 4.12: Scatterplots of predicted versus observed carbon

4.7. Carbon Stock mapping

Multiple linear regression models were used for both *Shorea robusta* and other species to estimate the amount of carbon stock and mapping the carbon stock in the study area. These models were chosen as RMSE% is the lowest compared to other models. Approximately 48973232.75 kg of carbon was estimated to be stored in woody biomass in the study area. The study area was of 547.44 ha thus the study area has approximately 89.45 MgCha⁻¹. The carbon map produced is shown in Figure 4.13. In the Figure, both insets (segments and Digital Camera image) are for the same area and inset (segments) shows the details of carbon stock per tree.

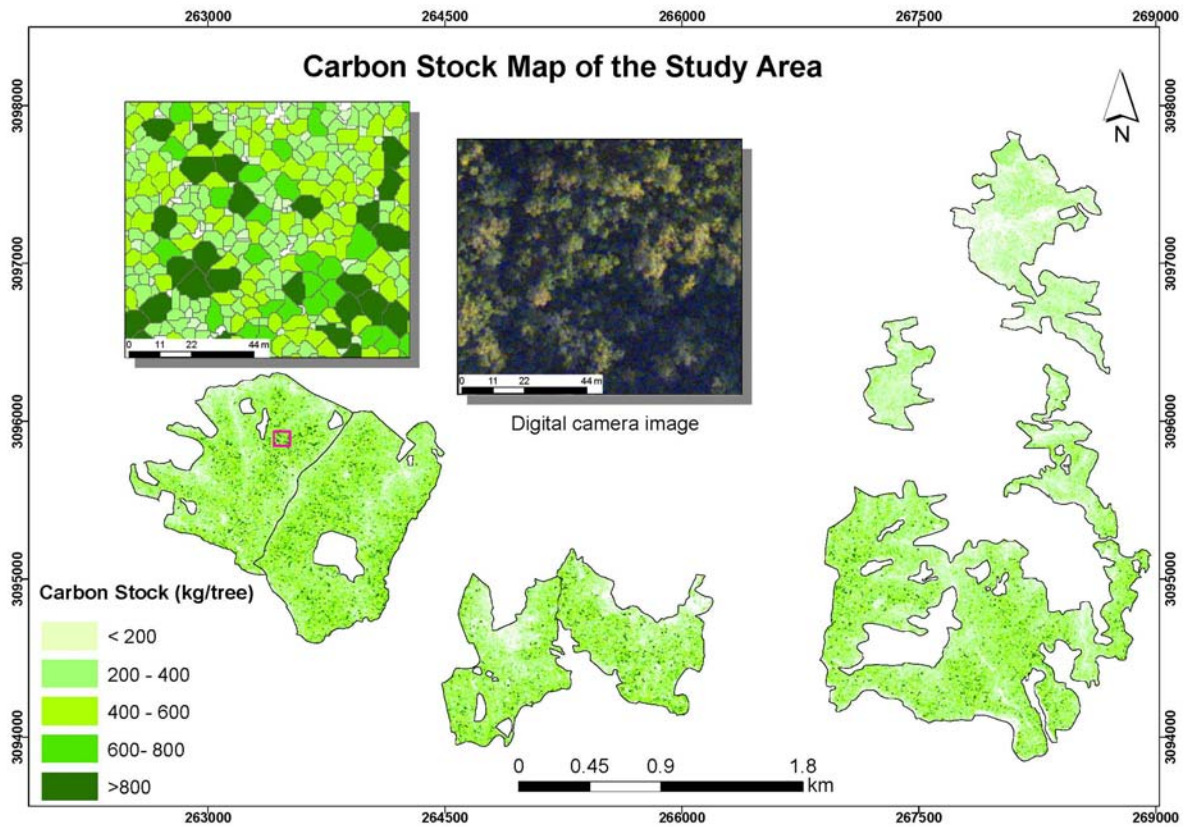


Figure 4.13: Carbon stock map of the study area and inset shows the details of carbon stock per tree

5. DISCUSSION

5.1. CHM preparation and accuracy assessment of LIDAR derived height

LIDAR derived tree height underestimated field measured tree height by 0.98 m on average. Comparison of LIDAR derived tree height with field measured tree height resulted to coefficient of determination (R^2) of 0.74 and RMSE was 2.8 m. The error could be because of low point density (0.8 point/m² on average). Due to the low point density, there is less probability that laser returns hit the true tree top of a tree. Some studies support this explanation. Saurez et al. (2005) demonstrated laser returns do not hit true tops of trees in the most common point densities such as 3-4 points/m². This leads to the variation in height measured from the field in this research. The underestimation of tree height for low point density was observed in various studies. For average point density of 2 points/m², Leckie et al. (2003) reported an average underestimation of ground measured tree height by 1.32 m and Saurez et al. (2005) found underestimation of ground measured tree height by 7-8% using airborne laser scanning (ALS) with point density of 3-4 point/m². Although these studies used higher point density compared to the data used in this study, their underestimation was higher. In both cases, the study area was in coniferous forests. The crowns of coniferous trees have a triangular shape (Figure 5.1a). Compare to this, the crowns of deciduous trees found in CFs of Ludikhola watershed are relatively flat leading to less variation in height from tree top to the edges of the crowns (Figure 5.1b). Due to the crown shape in coniferous trees, laser returns hitting the true tree top and those hitting the edges have a higher variation in height than in deciduous trees. Thus, in this study with low point density the underestimation is not high compared to the above mentioned studies.

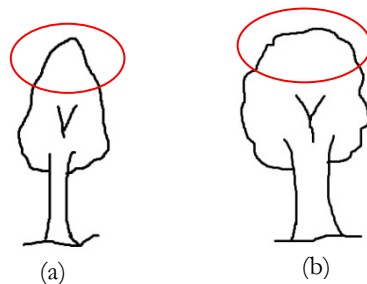


Figure 5.1: Crowns shape (a) coniferous tree (b) deciduous tree

LIDAR data products will be more accurate and precise with increase in point density (Heritage et al., 2009). According to Lefsky et al. (2002) point density is the main factor for height underestimation in discrete return of ALS data. However, point density might not be only the factor that affects LIDAR data products i.e. CHM. Study area of this research do not have 100% canopy cover. Thus, canopy height underestimation might be due to the laser pulse penetration into the canopy before reflecting a signal and the signal might not be detected by the scanner as a first return (Gaveau et al., 2003).

Apart from this, the gridding process might introduce error into the CHM through the interpolation method and the grid spacing chosen (Smith et al., 2004). Interpolation is needed as LIDAR gives point cloud with 'empty' spaces between points and there is no full area coverage like in optical systems. This means point clouds should be interpolated in order to convert the same coverage to an image. Beside this, field height measurement may have introduced errors (Brandtberg et al., 2003). During tree height measurements in the field, errors can be introduced by the field personnel which might cause the

difference between field measured and LIDAR derived height. In addition, sometime it is difficult to measure the highest point of the crown in deciduous forest as there is no distinct tree top. This was observed in the field when tree crowns were large with irregular shape. Field height measurement in such situation may introduce error.

5.2. Tree crown delineation and accuracy assessment

In this study, tree crown delineation was done using region growing approach which is explained in section 3.3.6 and results are presented in section 4.3.

Both images (CHM and Digital Camera image) were used in order to assign the classes trees and others (shadow, bare land). The use of CHM in this step helped to extract trees in shadow area (Figure 5.2) which would be missed if only reflectance values were used. However, it was noticed that the segments of tree crowns in the valleys were larger. There were big trees in the valleys. This is due to the better growth conditions in the valley area which was observed during the field work. The use of height information helped to separate trees from other vegetation (shrubs and herbs). In this regard, Leckie et al. (2003) found that the use of height information for tree crown delineation helped to eliminate most of the commission errors (delineating shrubs or other ground vegetation as trees) that often occur in open forest area with optical imagery.

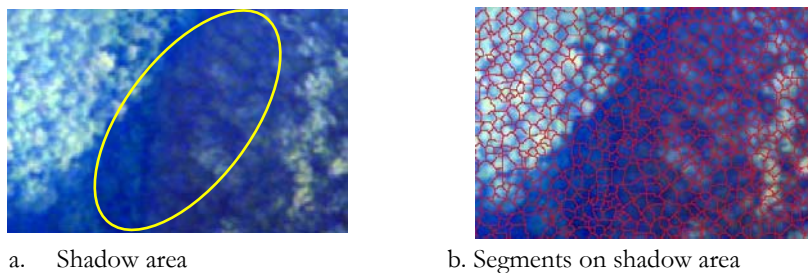
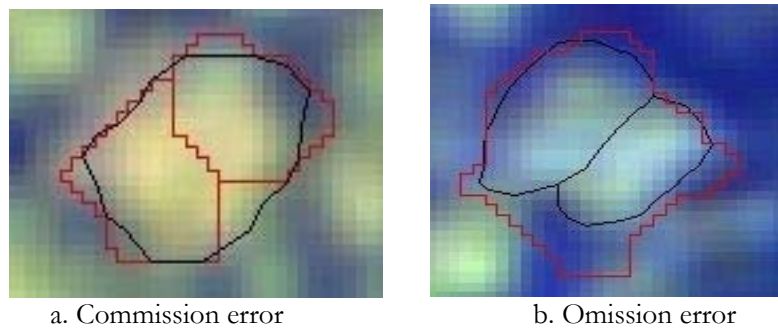


Figure 5.2: Digital camera image showing shadow area and segments on the shadow area

In this study, the segmentation result showed both commission and omission errors. In the study area, there are trees with different sizes ranging from DBH of 10 cm to 83 cm (based on field data collection). For the small tree crowns, the automated segments were matching with manually delineated crowns but for large tree crowns, there is often more group of automated segments. This means there were commission errors (Figure 5.3a). However, these errors were not observed for all large tree crowns. This might be because of irregular shape of the tree crown due to which an individual branch may create untrue tree tops, so there seems to be two trees instead of one. Similar case was observed by Chen et al. (2006) and explained that branches of big trees can reach far in different directions and grow into irregular shape. Then, the commission error occurs when each large branch is considered as a tree. Further, Leckie et al. (2003) stated that for a large tree, individual large branches of the tree can cause tree splitting. On the other hand, omission errors (Figure 5.3b) were also observed. This means the algorithm was not able to split the neighbouring trees and made one segment for two trees and in some part, one segment for three trees. This may be due to the low point density of LIDAR data and homogenous height distribution of neighbouring trees. In this regard, Koch et al. (2006) found that for deciduous trees, there were more omission errors which were due to the densely growing trees with homogenous height distribution leading to inability to separate neighbouring trees.



(Red polygons represent automated segments and black polygons represent manually delineated crowns)

Figure 5.3: Example of commission and omission error

Apart from these, distortion of digital camera image was observed (Figure 5.4) in some parts of the study area. Due to this, the algorithm in eCognition does not properly segment the tree crown.



Figure 5.4: Distortion in digital camera image

In this study, accuracy of tree crown delineation was 76.2% which is obtained based on matching of manually delineated tree crowns to automated segments and D value was 0.31. Shah (2011b) used region growing approach for tree crown delineation using high resolution Geocye image in Ludidamgade CF which is one of the CFs selected for the study in this research. In her study, accuracy of tree crown delineation was 68% with 1:1 correspondence. The segmentation accuracy is higher in this study compared to her study. The improvement in the segmentation could be due to the addition of height information for the segmentation. In this regard, Kim et al. (2010) also found better result of segmentation using LIDAR data and aerial photography than using either of the data alone.

5.3. Image classification and accuracy assessment

Overall classification accuracy achieved in this study was 75.86%. The user accuracy for *Shorea robusta* was 77% whereas for other species it was 71%. The user accuracy for *Shorea robusta* was higher because approximately 68% of the trees recognized in the field were *Shorea robusta*. The user accuracy in classifying other species is lower. This could be due to the smaller number of samples for training and validation. Moreover, all other species except *Shorea robusta* were grouped into one class as 'others'. Different species have their own spectral characteristics due to which there would be confusion in spectral response from the class 'others'.

The overall classification accuracy of this study is lower compared with Holmgren et al. (2008) who obtained 96% accuracy in classifying tree species into three groups when LIDAR data (50 points/m²) and

multi-spectral images (4 bands) were combined. In his study, several features such as canopy shape, height distribution, intensity of returns were extracted from LIDAR data. All these features were used for classification. In addition, his multispectral image had a near infrared band which is useful for vegetation classification. Compared to his research, this study used low point density LIDAR data and digital camera image without infrared band. Ali et al. (2008) achieved 86% overall classification accuracy for two species using multi-spectral imagery (4 bands) and LIDAR data (16 points/m²). The overall classification was more than 83% for three species obtained by Heinzl et al. (2008) using LIDAR data (7 points/m²) and aerial photographs (4 bands). Shah (2011b) obtained overall classification accuracy of 74% for two species (*Shorea robusta* and others) using Geoeye image in Ludidamgade CF, Gorkha, Nepal.

Beside these, there could be several factors that affect tree species classification. The digital camera image used in this study contained red green and blue bands. This image does not include NIR band although the band gives more information about vegetation than red, green and blue bands (ITC, 2010). This could affect the classification in this study. Effects of shadow could be another factor that affected the classification. Using LIDAR data, tree segments were extracted even from shadow area but for these segments brightness values were different from the trees located in non-shadow area for the same species which affects classification. In this regard, Leckie et al. (2005) found the effect of shadow on the tree species classification as the spectral information of the species was influenced by the shadow. His study was in old growth coniferous forest and used high resolution digital imagery.

Classification accuracy is also affected by segmentation quality (Ke et al., 2010). The higher classification accuracy will be obtained if the tree crown delineation is more precise. In this study, the classification could be influenced by the segmentation quality particularly omission and commission errors might create confusion in the classification as brightness value of those segments would be affected.

5.4. LIDAR data in separating intermingled tree crowns

The logic behind the hypothesis that LIDAR data can separate intermingled trees is based on the laser returns hitting the trees. If the laser has a sufficiently high point density, tree top (local maxima) and crown edge (local minima) for each tree will be detected and it should be able to separate intermingled trees based on height differences. In this study, this is not the case because of low point density. Due to this, laser returns do not hit exactly all tree tops of each individual tree and points (height value) are not enough to delineate the entire crown boundary (local minima). Points may fall besides the top at equal height, suggesting two tops exist or points may completely miss a top and only touch the edges.

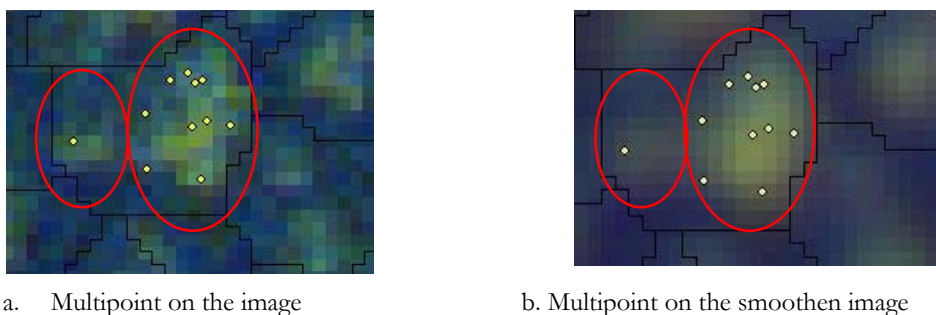


Figure 5.5: Showing multipoint (from point cloud) (red oval shapes show 2 trees that are intermingled)

In region growing segmentation, a region grows from the tree top until it reaches to the local minima. But here in intermingled trees as shown in Figure 5.5 there are two trees but there are not enough points with brightness values that are sufficiently different due to which the algorithm cannot separate two trees. Also,

points are irregularly spaced. However, this logic is only applicable for trees where there is a low degree of intermingling. Koch et al. (2006) found that for deciduous trees, there were more omission errors which were due to the densely growing trees with homogenous height distribution resulting in inability to separate neighbouring trees. He used the LIDAR data with point density of 5-10 points/m². In nature, trees can be intermingled in different degrees as shown in Figure 5.5. In this study, data about the degree of intermingled trees were not collected. If crowns have a high degree of intermingling there would be no local minima or valleys between tree tops and the crowns are considered to be one.

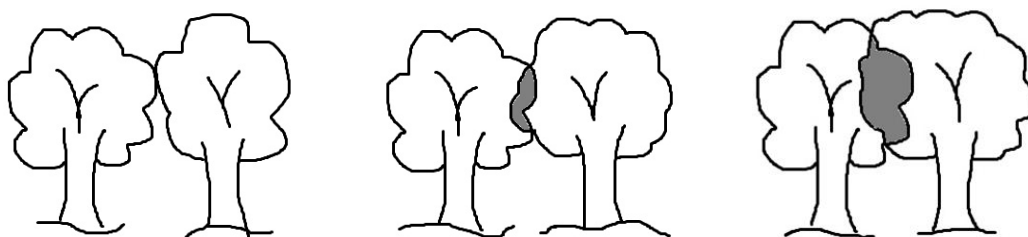


Figure 5.6: Different degree of two intermingled canopy trees

Beside this, CHM was developed from point clouds in an interpolation process which smoothens the data to some extent. Both Digital Camera image and CHM were filtered to smoothen. The degree of smoothing might affect tree crown delineation because the smoothing process blurs the maxima of a tree. Apparently, some studies (Reitberger et al., 2009; Solberg et al., 2006) showed that due to the CHM smoothing, two clear maxima for neighbouring trees were not visible due to which the trees were not separated. However, CHM smoothing is required to avoid the detection of several local maxima in one tree.

This study revealed that intermingled trees cannot be separated using LIDAR data with point density of 0.8 point/m². Nevertheless, if intermingled trees are homogenous in species composition, this might not affect considerably to the biomass estimation but if clusters of trees are heterogeneous, it might affect to the biomass estimation because wood density vary from species to species. In addition, small degree of intermingled trees might not affect considerably to the biomass estimation. However, high degree of intermingling might affect biomass estimation as intermingled trees might be delineated as a single tree (one segment). The intermixed portion of both the trees in the delineated crown is not considered due to which the delineated crown area is smaller than the sum of CPA of two trees in reality. This might underestimate the biomass of the trees.

5.5. Model development and validation

Linear relationship was found between CPA and carbon stock; height and carbon stock of the trees for both *Shorea robusta* and other species. The linear relationship was observed as most of the trees in the study area were young with mean DBH of 18 ± 8.7 cm and mean height of 12.6 ± 5.2 m. Mean DBH could be smaller than above mentioned if trees with DBH less than 10 cm had been measured in the field. Field observation showed that there was not competition between tree crowns in most of the cases because most of trees were young. During young age, DBH and crown increases linearly and later crown growth decreases as crown start touching each other (Shimano, 1997). Further, the use of non-linear model did not improve the coefficient of determination (R^2) hence considering the simplicity of model, simple linear model was preferred.

Coefficient of determination R^2 obtained for the relationship between CPA and carbon in the study were 0.62 for *Shorea robusta* and 0.61 for other species which is relatively low as compared to the result obtained by Shah (2011b). She used non-linear regression model to establish the relationship between CPA and

carbon and obtained R^2 of 0.67 for *Shorea robusta* and 0.7 for other species in Ludidamgade CF, Gorkha, Nepal. In this study, R^2 for the relationship between height and carbon were 0.64 and 0.63 for *Shorea robusta* and other species respectively which is comparable to the R^2 obtained by Yu et al. (2010). He obtained R^2 of 0.6 for a linear relationship between height and biomass in the mixed forest.

Multiple linear regression was followed in this study to derive the relationship of carbon with CPA and height. Popescu (2007) used multiple linear regression to derived DBH using LIDAR derived crown diameter and height and then estimated biomass using derived DBH. Adjusted R^2 for the model were 0.72 and 0.65 for *Shorea robusta* and other species respectively. This means 72% of the variation in carbon can be explained by CPA and height for *Shorea robusta* and 65% of the variation of carbon can be explained by CPA and height for other species. The relationship was improved when two variables were used for *Shorea robusta* but for other species there was not much improvement. This could be due to the mixing of different trees species in the class 'others' due to which there were variation in CPA and height.

The lowest RMSE% i.e. 36.8% and 32.4% was obtained in case of multiple linear regression for both *Shorea robusta* and other species. This shows that there were 36.8% average error in the prediction of the carbon stock for *Shorea robusta* and 32.4% average error in the prediction of the carbon stock for other species. The result showed that there were improvements in the models using two explanatory variables (CPA and height). Height and CPA are important biophysical parameters to estimate biomass of a tree using remote sensing. Moreover, biomass depends on volume and volume can be calculated from height and DBH. Since there is relation between CPA and DBH (Hirata et al., 2009; Shimano, 1997), it is expected that CPA and height will give a good estimate of biomass. Consequently these two variables i.e. height and CPA can explain more about variability of biomass than using either of variables alone.

RMSE% was 47.1% and 41.5% for *Shorea robusta* and other species respectively in modelling the relationship of carbon and CPA whereas it was 40.3% and 35.3% respectively in modelling the relationship of carbon and height. This shows height seems to explain variation in biomass better than CPA. This was expected because biomass of a tree is acquired mainly from stem part than from CPA and height is one of the main parameters to estimate volume (stem part) of a tree.

Multiple regression models were used for both *Shorea robusta* and other species to calculate carbon stock in the study area since they had the lowest RMSE%. The model performance was relatively poorer for small trees because of high negative intercept in the models. There are two possible reasons for the negative intercept in the regression model. Firstly, model parameters derived from LIDAR data and Digital Camera image (height and CPA) were used to estimate the biomass of a tree and found some discrepancies between field-measured model parameter (height) and remotely sensed model parameter (height). Secondly, the dataset that was used for the calibration of model did not include the small size trees.

Biomass estimation was done after several steps from field data collection to model development. During the various processes, errors could be introduced and propagated to the model development which could be the reasons for the obtained RMSE%. Sources of errors affecting the biomass estimation are described in detail in section 5.7.

5.6. Biomass and carbon stock estimation

In this study, approximately 89.45 MgCha^{-1} of carbon stock was estimated for the study area which is lower compared to results of Baral et al. (2010) who found 99.43 MgCha^{-1} of above-ground carbon stock in *Shorea robusta* forest of hilly region in Nepal. Jamarkattel (2011) obtained 70 MgCha^{-1} in a study done in CFs where *Shorea robusta* is the dominant species. Compared to this study, she obtained lesser carbon

stock. This could be because of masking shadow area in her study due to which all the trees in the shadow area were not counted resulting in smaller number of trees whereas in this study trees in the shadow area were also considered. This would affect the total number of trees in the study area and eventually the carbon stocks.

5.7. Sources of error or uncertainties

5.7.1. Allometric equation

The accuracy of allometric equation affects the accuracy of the model (García et al., 2010). The allometric equation developed for one area may introduce error when it is used for a different area. Site specific and species specific allometric equations are essential to accurately estimate biomass of the forest. The major sources of uncertainty are the coefficient parameters 'a' and 'b' in allometric equation when they are not calibrated for a specific site (Ketterings et al., 2001).

The study area of this research was in the sub-tropical region. However, the allometric equation used in this study is for tropical moist forest. Thus, one of the sources of error in biomass estimation could be the allometric equation.

5.7.2. Unsystematic shift between LIDAR data and Digital camera imagery

Unsystematic shift of 0-1 m was observed i.e. spatial overlap between two datasets was not exactly matching. This shift might be due to different sensors for LIDAR data and Digital Camera imagery. The average crown diameter of trees is approximately 4 m and comparing with the size of trees, the shift was acceptable. However, the shift might affect the derived parameters CPA and height which would affect in the estimation of carbon stock.

5.7.3. Other errors/uncertainty

Errors and uncertainties can be introduced at any step from data and operations which are then accumulated and propagated to the maps (Wang et al., 2005). There were mainly four major operations in this study and in each operation, error could be introduced.

The first step was CHM derivation from LIDAR point cloud. Coefficient of determination (R^2) of 0.74 was obtained from the comparison between LIDAR derived height and field height. This shows 74% of variation in the field height can be explained by the LIDAR derived height and RMSE was 2.8 m. This error can accumulate and propagate in the further step.

The next step was segmentation. The segmentation accuracy showed there were errors. Commission and omission errors were observed due to overlapping trees and branches of big trees which can reach far in different directions and grow into irregular shape. These errors can propagate in the further step.

The next operation was classification of tree species. When classification is not correct, accurate estimation of biomass is not possible. Error in classification may lead to selection of wrong wood specific gravity for a tree. Error in classification could be due to spectral characteristic of vegetation, shadows, distortion of the image and misidentification of tree.

The last operation was model development. Selection of appropriate model is required. Data used for the model should be good representative of population (trees) in the study area. Otherwise, this might affect the model. Beside these, errors from allometric equation would affect the model.

Apart from these, field measurements might have errors. Errors could be aroused from sampling error, improper measurement of DBH and height. In this regard, Gonzalez et al. (2010) studied the uncertainty of field measurements and found high uncertainty on these measurements. All these errors propagated to the models. Finally, the errors affect the carbon estimation and mapping.

Figure 5.7 shows the diagrammatic representation of errors and their propagations into the final map. Estimation of magnitude of these errors and the error propagations in the study is beyond the scope of the study but it is necessary to understand why the accuracy of the carbon stock estimation is relatively is low. Although there are sources of errors, this research focuses on development of a method but not for a perfect carbon mapping application. However, the research also makes aware that there are sources of error which require further study.

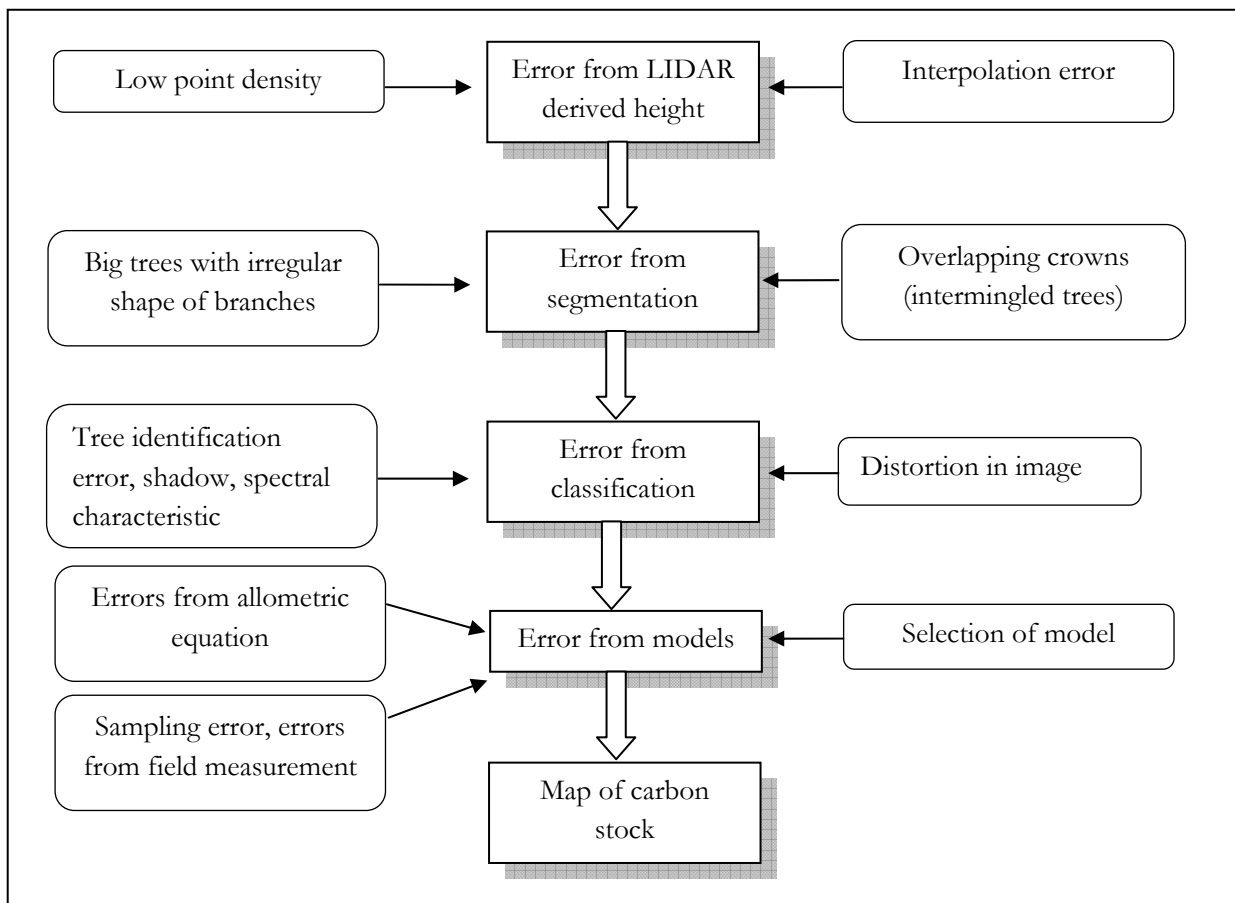


Figure 5.7: Sources of errors and their accumulation and propagation into the map

6. CONCLUSIONS AND RECOMMENDATIONS

A significant relationship of carbon with CPA and height was found which improves carbon stock estimation. The method applied in this study which includes the integration of LIDAR data and high resolution Digital Camera imagery, can be used for carbon stock estimation. Following conclusions were drawn for each research question.

6.1. Conclusions

What is the accuracy of tree crown delineation using LIDAR data and Digital Camera imagery?

The overall accuracy of tree crown delineation was 76.2% and D value was 0.31.

How effective is LIDAR data in separating intermingled tree crowns?

Intermingled tree crowns were not separated using LIDAR data with average point density of 0.8 point/m².

Is there any multicollinearity between CPA and height?

The correlation between CPA and height for both *Shorea robusta* and other species were checked. The correlation coefficient for *Shorea robusta* was 0.58 and Variance inflation factor (VIF) was 1.51 whereas for other species correlation coefficient was 0.34 and VIF was 1.13. This shows that the degree of multicollinearity was very low. This indicates that there was no effect of multicollinearity on the model.

Which model has the highest accuracy for carbon estimation?

The models including both height and CPA has higher accuracy in carbon estimation compared to the model including only CPA and the model including only height. In order to derive the relationship of carbon with CPA and height, multiple linear regressions models were developed for both *Shorea robusta* and other species. These models had the lowest RMSE% i.e. 36.8% and 32.4% for both *Shorea robusta* and other species respectively.

What is the amount of carbon stock in the study area?

The total amount of carbon stock in the study area was approximately 48973Mg which was 89.45MgCha⁻¹.

Related to the general objective - to develop a method to accurately estimate and map above ground carbon stocks using airborne LIDAR data and high resolution Digital Camera imagery:

Although the models developed suffer from 36.8% (*Shorea robusta*) and 32.4% (others) of error percentage, this study shows that it is feasible to estimate and map above ground carbon stocks using airborne LIDAR data and high resolution Digital Camera imagery though it has some limitations. The main limitation is trees species were classified into only two classes and less number of sample sizes was used for model calibration and validation. Multiple regression models developed in this study did not perform well for small trees. Improvement can be on done by classifying more tree species and developing species wise regression models using more number of observations which include all sizes of trees.

6.2. Recommendations

- The allometric equation used in this study was not site specific which will bring errors in the developed models. Therefore, there is a need to develop site specific and species specific allometric equations for Nepal for accurate carbon stock estimation.
- There should be sufficient number of observations for each tree species. This will help to classify tree species and then develop species wise model of CPA, height and biomass relationship. Sufficient sample size should be used to develop models. This will make the models more reliable and improved.
- In this study, due to the low point density LIDAR data, intermingled trees were not separated. Therefore, it is recommended to use relatively high point density LIDAR data and assessment should be done whether the intermingled trees are separated or not. Further, data about degree of intermingled trees should be collected. This may help to analyse the result in the sense that if the trees are separated then, up to which degree of intermingle it can separate and for which degree of intermingle it cannot separate.
- The method developed in this study can be applied using relatively high point density LIDAR data and digital camera imagery. It is recommended to analyse the added value of using high point density LIDAR data in segmentation and tree species classification.

LIST OF REFERENCES

- Acharya, K. P., Dang, R. B., Tripathi, D. M., Bushley, B. R., Bhandary, R. R., & Bhattarai, B. (2009). *Ready for REDD? Taking Stock of Experiences, Opportunities and Challenges in Nepal*. Kathmandu, Nepal: Nepal Foresters' Association.
- Ali, S. S., Dare, P., & Jones, S. D. (2008). Fusion of remotely sensed multispectral imagery and lidar data for forest structure assessment at the tree level. *The International Archives of the Photogrammetry, Remote Sensing and Spatial Information Sciences*, XXXVII(Part B7).
- Baccini, A., Friedl, M. A., Woodcock, C. E., & Warbington, R. (2004). Forest biomass estimation over regional scales using multisource data. *Geophysical Research Letters*, 31(10).
- Baral, S., Malla, R., & Ranabhat, S. (2010). Above-ground carbon stock assessment in different forest types of Nepal. *Banko Janakari*, 19(2), 10-14.
- Blaschke, T., Burnett, C., & Pekkarinen, A. (2006). Image segmentation methods for object-based analysis and classification. *Remote sensing image analysis: Including the spatial domain*, 211-236.
- Brandtberg, T., Warner, T. A., Landenberger, R. E., & McGraw, J. B. (2003). Detection and analysis of individual leaf-off tree crowns in small footprint, high sampling density lidar data from the eastern deciduous forest in North America. *Remote Sensing of Environment*, 85(3), 290-303.
- Brown, S. (2002). Measuring carbon in forests: current status and future challenges. *Environmental Pollution*, 116(3), 363-372.
- Chave, J., Andalo, C., Brown, S., Cairns, M., Chambers, J., Eamus, D., et al. (2005). Tree allometry and improved estimation of carbon stocks and balance in tropical forests. *Oecologia*, 145(1), 87-99.
- Chen, L., Chiang, T., & Teo, T. (2005). *Fusion of LIDAR data and high resolution images for forest canopy modelling*.
- Chen, Q., Baldocchi, D., Gong, P., & Kelly, M. (2006). Isolating individual trees in a savanna woodland using small footprint lidar data. *Photogrammetric engineering and remote sensing*, 72(8), 923-932.
- Clinton, N., Holt, A., Scarborough, J., Yan, L., & Gong, P. (2010). Accuracy assessment measures for object-based image segmentation goodness. *Photogrammetric engineering and remote sensing*, 76(3), 289-299.
- Culvenor, D. S. (2002). TIDA: an algorithm for the delineation of tree crowns in high spatial resolution remotely sensed imagery. *Computers & Geosciences*, 28(1), 33-44.
- Definiens. (2007). *Definiens Developer 7: Reference Book*. Munich, Germany.
- DFRS. (1999). *Forest Resources of Nepal (1987-1998)*: Ministry of Forests and Soil Conservation, Forest Survey Division, Kathmandu, Nepal.
- Dhital, N. (2009). Reducing Emissions from Deforestation and Forest Degradation (REDD) in Nepal: Exploring the Possibilities. *Journal of Forest and Livelihood*, 8(1), 57-62.
- Dixon, R. K., Winjum, J. K., & Schroeder, P. E. (1993). Conservation and sequestration of carbon : The potential of forest and agroforest management practices. *Global Environmental Change*, 3(2), 159-173.
- DOF. (2004). *Community Forestry Inventory Guidelines*: Community Forest Division, Department of Forests, Kathmandu, Nepal.
- Dong, J., Kaufmann, R. K., Myneni, R. B., Tucker, C. J., Kauppi, P. E., Liski, J., et al. (2003). Remote sensing estimates of boreal and temperate forest woody biomass: carbon pools, sources, and sinks. *Remote Sensing of Environment*, 84(3), 393-410.
- Drake, J. B., Knox, R. G., Dubayah, R. O., Clark, D. B., Condit, R., Blair, J. B., et al. (2003). Above-ground biomass estimation in closed canopy Neotropical forests using lidar remote sensing: factors affecting the generality of relationships. *Global Ecology and Biogeography*, 12(2), 147-159.
- DSCO. (2006). *The Sub-watershed Management Plan, Lumdi Khola Sub-watershed of Gorkha*. Gorkha, Nepal.
- Dubayah, R. O., & Drake, J. B. (2000). Lidar remote sensing for forestry. *Journal of forestry*, 98(6), 44-46.
- eCognition. (2011a). *eCognition Developer 8.7 : Reference Book*. Munich, Germany.
- eCognition. (2011b). *eCognition Developer 8.7 : User Guide*. Munich, Germany.
- FAO. (2004b). National forest inventory: Field manual Template. Retrieved 21 august, 2011, from <http://www.fao.org/docrep/008/ae578e/ae578e00.htm>
- García, M., Riaño, D., Chuvieco, E., & Danson, F. M. (2010). Estimating biomass carbon stocks for a Mediterranean forest in central Spain using LiDAR height and intensity data. *Remote Sensing of Environment*, 114(4), 816-830.

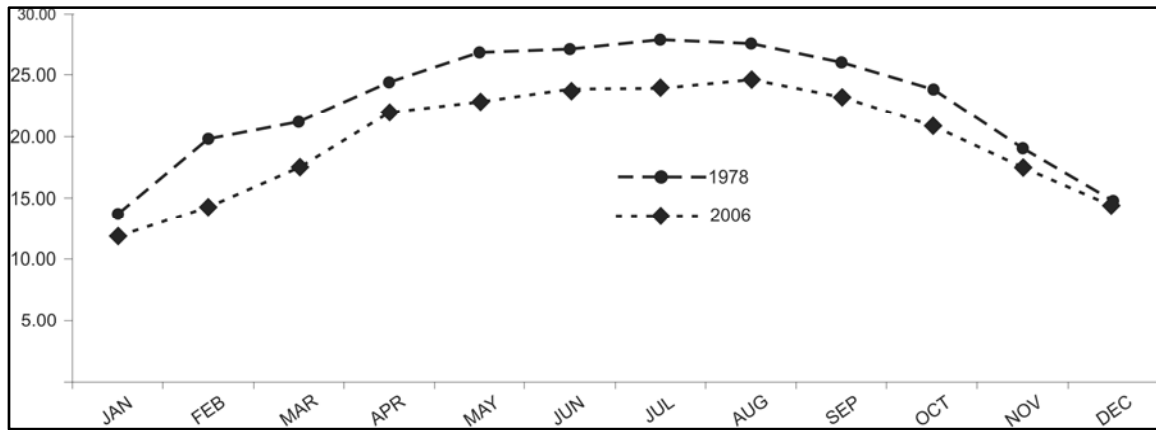
- Gaveau, D. L. A., & Hill, R. A. (2003). Quantifying canopy height underestimation by laser pulse penetration in small-footprint airborne laser scanning data. *Canadian Journal of Remote Sensing*, 29(5), 650-657.
- Gibbs, H. K., Brown, S., Niles, J. O., & Foley, J. A. (2007). Monitoring and estimating tropical forest carbon stocks: making REDD a reality. *Environmental Research Letters*, 2(4).
- Gonzalez, P., Asner, G. P., Battles, J. J., Lefsky, M. A., Waring, K. M., & Palace, M. (2010). Forest carbon densities and uncertainties from Lidar, QuickBird, and field measurements in California. *Remote Sensing of Environment*, 114(7), 1561-1575.
- Gschwantner, T., Schadauer, K., Vidal, C., Lanz, A., Tomppo, E., di Cosmo, L., et al. (2009). Common tree definitions for national forest inventories in Europe. *Silva Fennica*, 43(2), 303-321.
- Heinzel, J. N., Weinacker, H., & Koch, B. (2008). *Full automatic detection of tree species based on delineated single tree crowns-a data fusion approach for airborne laser scanning data and aerial photographs*. Paper presented at the SilviLaser.
- Heritage, G. L., & Large, A. R. G. (2009). *Laser Scanning for the Environmental Sciences*. Chichester, UK: Wiley-Blackwell Publishing Ltd.
- Hirata, Y., Tsubota, Y., & Sakai, A. (2009). Allometric models of DBH and crown area derived from QuickBird panchromatic data in *Cryptomeria japonica* and *Chamaecyparis obtusa* stands. *International Journal of Remote Sensing*, 30(19), 5071-5088.
- Holmgren, J., Persson, Å., & Söderman, U. (2008). Species identification of individual trees by combining high resolution LiDAR data with multi-spectral images. *International Journal of Remote Sensing*, 29(5), 1537-1552.
- Hug, C., Krzystek, P., & Fuchs, W. (2004). Advanced lidar data processing with LasTools. *International Archives of Photogrammetry and Remote Sensing*, 35.
- Hunt, C. A. G. (2009). *Carbon sinks and climate change: forests in the fight against global warming*. Cheltenham, United Kingdom: Edward Elgar Publishing Limited.
- Husch, B., Beers, T. W., & Kershaw, J. A. (2003). *Forest mensuration*. Hoboken, New Jersey: John Wiley & Sons, Inc.
- Hyyppä, J., Pyysalo, U., Hyyppä, H., & Samberg, A. (2000). *Elevation accuracy of laser scanning-derived digital terrain and target models in forest environment*.
- ICIMOD, ANSAB, & FECOFUN. (2010). *Report on forest carbon stocks in Ludikhola, Kayarkhola and Charnawati Watersheds of Nepal*. Kathmandu, Nepal.
- IPCC. (2003). *Good Practice Guidance for Land Use, Land Use Change and Forestry*. Hayama, Kanagawa, Japan.
- IPCC. (2007). Summary for Policymakers. In: *Climate Change 2007: The Physical Science Basis. Contribution of Working Group I to the Fourth Assessment Report of the Intergovernmental Panel on Climate Change* [Solomon, S., D. Qin, M. Manning, Z. Chen, M. Marquis, K.B. Averyt, M. T. and H.L. Miller] (Eds.) (pp. 2). Cambridge, United Kingdom: Cambridge University Press.
- ITC. (2010). *GI Science and Earth Observation: a process-based approach*. Enschede, The Netherlands: ITC.
- Jamarkattel, S. (2011). *Mapping carbon stock using high resolution satellite images in sub-tropical forest of Nepal*. MSc thesis, University of Twente, Faculty of Geo-Information and Earth Observation ITC, Enschede.
- Jenkins, J. C., Chojnacky, D. C., Heath, L. S., & Birdsey, R. A. (2003). National-scale biomass estimators for United States tree species. *Forest Science*, 49(1), 12-35.
- Katoh, M., Gougeon, F., & Leckie, D. (2009). Application of high-resolution airborne data using individual tree crowns in Japanese conifer plantations. *Journal of Forest Research*, 14(1), 10-19.
- Ke, Y., Quackenbush, L. J., & Im, J. (2010). Synergistic use of QuickBird multispectral imagery and LIDAR data for object-based forest species classification. *Remote Sensing of Environment*, 114(6), 1141-1154.
- Ketterings, Q. M., Coe, R., van Noordwijk, M., Ambagau, Y., & Palm, C. A. (2001). Reducing uncertainty in the use of allometric biomass equations for predicting above-ground tree biomass in mixed secondary forests. *Forest Ecology and Management*, 146(1-3), 199-209.
- Kim, S. R., Kwak, D. A., Lee, W. K., Son, Y., Bae, S. W., Kim, C., et al. (2010). Estimation of carbon storage based on individual tree detection in *Pinus densiflora* stands using a fusion of aerial photography and LiDAR data. *Science China-Life Sciences*, 53(7), 885-897.
- Koch, B., Heyder, U., & Weinacker, H. (2006). Detection of individual tree crowns in airborne lidar data. *Photogrammetric engineering and remote sensing*, 72(4), 357.
- Lamichhane, B. R., & Awasthi, K. D. (2009). Changing Climate in a Mountain Sub-watershed in Nepal. *Journal of Forest and Livelihood*, 8(1), 99-105.

- Leckie, D., Gougeon, F., Hill, D., Quinn, R., Armstrong, L., & Shreenan, R. (2003). Combined high-density lidar and multispectral imagery for individual tree crown analysis. *Canadian Journal of Remote Sensing*, 29(5), 633-649.
- Leckie, D. G., Gougeon, F. A., Tinis, S., Nelson, T., Burnett, C. N., & Paradine, D. (2005). Automated tree recognition in old growth conifer stands with high resolution digital imagery. *Remote Sensing of Environment*, 94(3), 311-326.
- Lefsky, M. A., Cohen, W. B., Parker, G. G., & Harding, D. J. (2002). Lidar remote sensing for ecosystem studies. *Bioscience*, 52(1), 19-30.
- Lillesand, T. M., Kiefer, R. W., & Chpman, J. W. (2008). *Remote sensing and image interpretation* (Sixth ed.). New York: Wiley & Sons.
- Lim, K., Treitz, P., Wulder, M., St-Onge, B., & Flood, M. (2003). LiDAR remote sensing of forest structure. *Progress in Physical Geography*, 27(1), 88-106.
- Lu, D., Mausel, P., Brondízio, E., & Moran, E. (2004). Relationships between forest stand parameters and Landsat TM spectral responses in the Brazilian Amazon Basin. *Forest Ecology and Management*, 198(1-3), 149-167.
- Lu, D. S. (2006). The potential and challenge of remote sensing-based biomass estimation. *International Journal of Remote Sensing*, 27(7), 1297-1328.
- Massada, A., Carmel, Y., Tzur, G. E., Grunzweig, J. M., & Yakir, D. (2006). Assessment of temporal changes in aboveground forest tree biomass using aerial photographs and allometric equations. *Canadian Journal of Forest Research-Revue Canadienne De Recherche Forestiere*, 36(10), 2585-2594.
- MOFSC. (2009a). REDD-Forestry and Climate Change Cell. Retrieved 20 July, 2011, from <http://mofsc-redd.gov.np/introduction/>
- MOFSC. (2009b). REDD-Forestry and Climate Change Cell. Retrieved 20 November, 2011, from <http://mofsc-redd.gov.np/introduction/>
- Möller, M., Lymburner, L., & Volk, M. (2007). The comparison index: A tool for assessing the accuracy of image segmentation. *International Journal of Applied Earth Observation and Geoinformation*, 9(3), 311-321.
- Mora, B., Wulder, M. A., & White, J. C. (2010). Segment-constrained regression tree estimation of forest stand height from very high spatial resolution panchromatic imagery over a boreal environment. *Remote Sensing of Environment*, 114(11), 2474-2484.
- Muukkonen, P., & Heiskanen, J. (2007). Biomass estimation over a large area based on standwise forest inventory data and ASTER and MODIS satellite data: A possibility to verify carbon inventories. *Remote Sensing of Environment*, 107(4), 617-624.
- Naesset, E. (1997). Determination of mean tree height of forest stands using airborne laser scanner data. *ISPRS Journal of Photogrammetry and Remote Sensing*, 52(2), 49-56.
- Obrien, R. (2007). A Caution Regarding Rules of Thumb for Variance Inflation Factors. *Quality & Quantity*, 41(5), 673-690.
- Oli, B. N., & Shrestha, K. (2009). Carbon Status in Forests of Nepal: An Overview. *Journal of Forest and Livelihood*, Vol 8 (1), 62-67.
- Palace, M., Keller, M., Asner, G. P., Hagen, S., & Braswell, B. (2008). Amazon forest structure from IKONOS satellite data and the automated characterization of forest canopy properties. *Biotropica*, 40(2), 141-150.
- Patenaude, G., Milne, R., & Dawson, T. P. (2005). Synthesis of remote sensing approaches for forest carbon estimation: reporting to the Kyoto Protocol. *Environmental Science & Policy*, 8(2), 161-178.
- Phillips, O. L., Malhi, Y., Vinceti, B., Baker, T., Lewis, S. L., Higuchi, N., et al. (2002). Changes in growth of tropical forests: Evaluating potential biases. *Ecological Applications*, 12(2), 576-587.
- Popescu, S. C. (2007). Estimating biomass of individual pine trees using airborne lidar. *Biomass and Bioenergy*, 31(9), 646-655.
- Popescu, S. C., & Wynne, R. H. (2004). Seeing the trees in the forest: using lidar and multispectral data fusion with local filtering and variable window size for estimating tree height. *Photogrammetric engineering and remote sensing*, 70(5), 589-604.
- Pouliot, D., King, D., Bell, F., & Pitt, D. (2002). Automated tree crown detection and delineation in high-resolution digital camera imagery of coniferous forest regeneration. *Remote Sensing of Environment*, 82(2), 322-334.
- REDD. (2011). Community REDD working area. Retrieved 15 november, 2011, from <http://communityredd.net/>

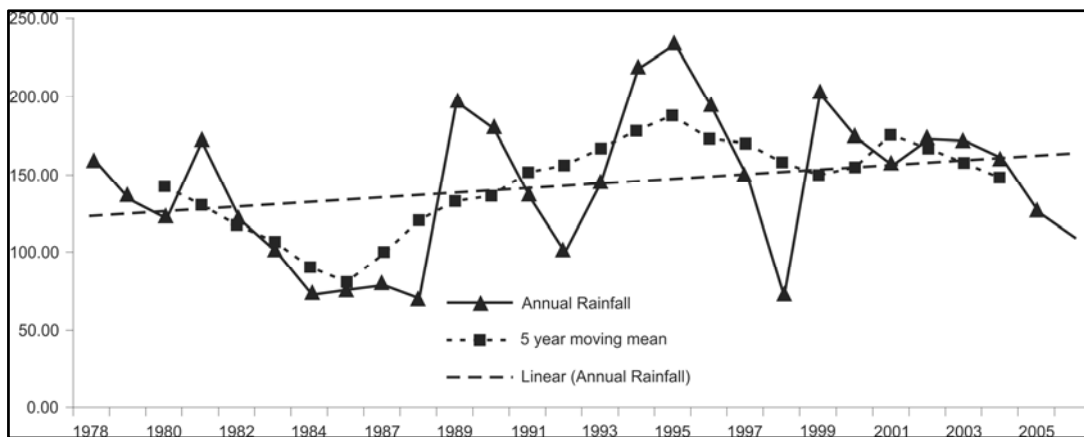
- Reitberger, J., Heurich, M., Krzystek, P., & Stilla, U. (2007). Single tree detection in forest areas with high-density LiDAR data. *International Archives of Photogrammetry, Remote Sensing and Spatial Information Sciences*, 36, 139-144.
- Reitberger, J., Schnörr, C., Krzystek, P., & Stilla, U. (2009). 3D segmentation of single trees exploiting full waveform LIDAR data. *ISPRS Journal of Photogrammetry and Remote Sensing*, 64(6), 561-574.
- Shah, R. (2011b). *Comparison of individual tree crown delineation method for carbon stock estimation using very high resolution satellite images*. MSc thesis, University of Twente Faculty of Geo-Information and Earth Observation ITC, Enschede.
- Shimano, K. (1997). Analysis of the relationship between DBH and crown projection area using a new model. *Journal of Forest Research*, 2(4), 237-242.
- Shrestha, S. K. (2011). *Carbon stock estimation using very high resolution satellite imagery and individual crown segmentation : a case study of broadleaved and needle leaved forest of Dollakha, Nepal*. MSc thesis, University of Twente, Faculty of Geo-Information and Earth Observation ITC, Enschede.
- Smith, S., Holland, D., & Longley, P. (2004). *The importance of understanding error in lidar digital elevation models*.
- Solberg, S., Naesset, E., & Bollandsas, O. M. (2006). Single tree segmentation using airborne laser scanner data in a structurally heterogeneous spruce forest. *Photogrammetric engineering and remote sensing*, 72(12), 1369.
- Song, C., Dickinson, M. B., Su, L., Zhang, S., & Yaussey, D. (2010). Estimating average tree crown size using spatial information from Ikonos and QuickBird images: Across-sensor and across-site comparisons. *Remote Sensing of Environment*, 114(5), 1099-1107.
- Steininger, M. K. (2000). Satellite estimation of tropical secondary forest above-ground biomass: data from Brazil and Bolivia. *International Journal of Remote Sensing*, 21(6-7), 1139-1157.
- Suárez, J. C., Ontiveros, C., Smith, S., & Snape, S. (2005). Use of airborne LiDAR and aerial photography in the estimation of individual tree heights in forestry. *Computers & Geosciences*, 31(2), 253-262.
- Thenkabail, P. S., Enclona, E. A., Ashton, M. S., Legg, C., & De Dieu, M. J. (2004). Hyperion, IKONOS, ALI, and ETM+ sensors in the study of African rainforests. *Remote Sensing of Environment*, 90(1), 23-43.
- Tritton, L. M., & Hornbeck, J. W. (1982). *Biomass equations for major tree species in the Northeast*: United States Forest Service.
- Tsendbazar, N. E. (2011). *Object based image analysis of geo - eye VHR data to model above ground carbon stock in Himalayan mid - hill forests, Nepal*. MSc thesis, University of Twente, Faculty of Geo-Information and Earth Observation ITC, Enschede.
- U.S. EPA. (2011). Climate Change-Greenhouse Gas Emissions. Retrieved 21 July, 2011, from <http://www.epa.gov/climatechange/emissions/co2.html>
- UNEP. (1999). Chapter 2: the state of the environment in Global Environment Outlook 2000. Complete Report. Retrieved 27 May, 2011, from <http://www.unep.org/geo/GEO2000/english/text/0040.htm>
- UNFCCC. (1997). Kyoto Protocol. Retrieved 26 May, 2011, from http://unfccc.int/kyoto_protocol/items/3145.php
- UNFCCC. (2007). Part Two: Action taken by the Conference of the Parties at its thirteenth session Retrieved 28 May 2011, from http://unfccc.int/methods_science/redd/items/4531.php
- Wang, G., Gertner, G. Z., Fang, S., & Anderson, A. (2005). A methodology for spatial uncertainty analysis of remote sensing and GIS products. *Photogrammetric engineering and remote sensing*, 71(12), 1423.
- Yadav, N. P. (2004). *Forest user groups in Nepal: Impacts on community forest management and community development* PhD thesis, The University of Leeds, Schools of Geography, U.K.
- Yu, Y., Saatchi, S., Heath, L. S., LaPoint, E., Myneni, R., & Knyazikhin, Y. (2010). Regional distribution of forest height and biomass from multisensor data fusion. *J. Geophys. Res*, 115, G00E12.
- Zhan, Q., Molenaar, M., Tempfli, K., & Shi, W. (2005). Quality assessment for geospatial objects derived from remotely sensed data. *International Journal of Remote Sensing*, 26(14), 2953-2974.
- Zhang, X. Y., Feng, X. Z., & Jiang, H. (2010). Object-oriented method for urban vegetation mapping using IKONOS imagery. *International Journal of Remote Sensing*, 31(1), 177-196.
- Zhang, Y. J. (1996). A survey on evaluation methods for image segmentation. *Pattern recognition*, 29(8), 1335-1346.

APPENDICES

Appendix 1: (a) Average monthly temperature of 1978 and 2006 (b) Rainfall trend from 1978-2006 source: (Lamichhane et al., 2009)



(a)



(b)

Appendix 2: List of tree species found in the study area

S.N	Local name	Scientific name
1	Sal	<i>Shorea robusta</i>
2	Chilaune	<i>Schima wallichii</i>
3	Bhalayo	<i>Rhus wallichii</i>
4	Barro	<i>Terminalia bellirica</i>
5	Aap	<i>Mangifera indica</i>
6	Kyamuna	<i>Cleistocalyx operculata</i>
7	Karam	<i>Adina cordifolia</i>
8	Saaj	<i>Terminalia alata</i>
9	Kumbho	<i>Cochlospermum religiosum</i>
10	Januma	<i>Syzygium cumini</i>
11	Katus	<i>Castanopsis indica</i>
12	sallo	<i>Pinus roxburghii</i>
13	Khirro	<i>Sapium insigne</i>
14	Bot Dhayaro	<i>Lagerstroemia parviflora</i>
15	Mainkanda	<i>Xeromphis spinosa</i>
16	Khaniyo	<i>Ficus semicordata</i>
17	Kaiyo	<i>Wendlandia puberula</i>
18	Mauwa	<i>Engelhardia spicata</i>
19	Amaro	<i>Spondias pinnata</i>
20	Chuwa	<i>Phlogacanthus byrsiflorus</i>
21	Putalikath	
22	Anger	
23	Dungre	
24	Kuhelo	
25	Panchpate	
26	Taniyo	
27	Khallo	

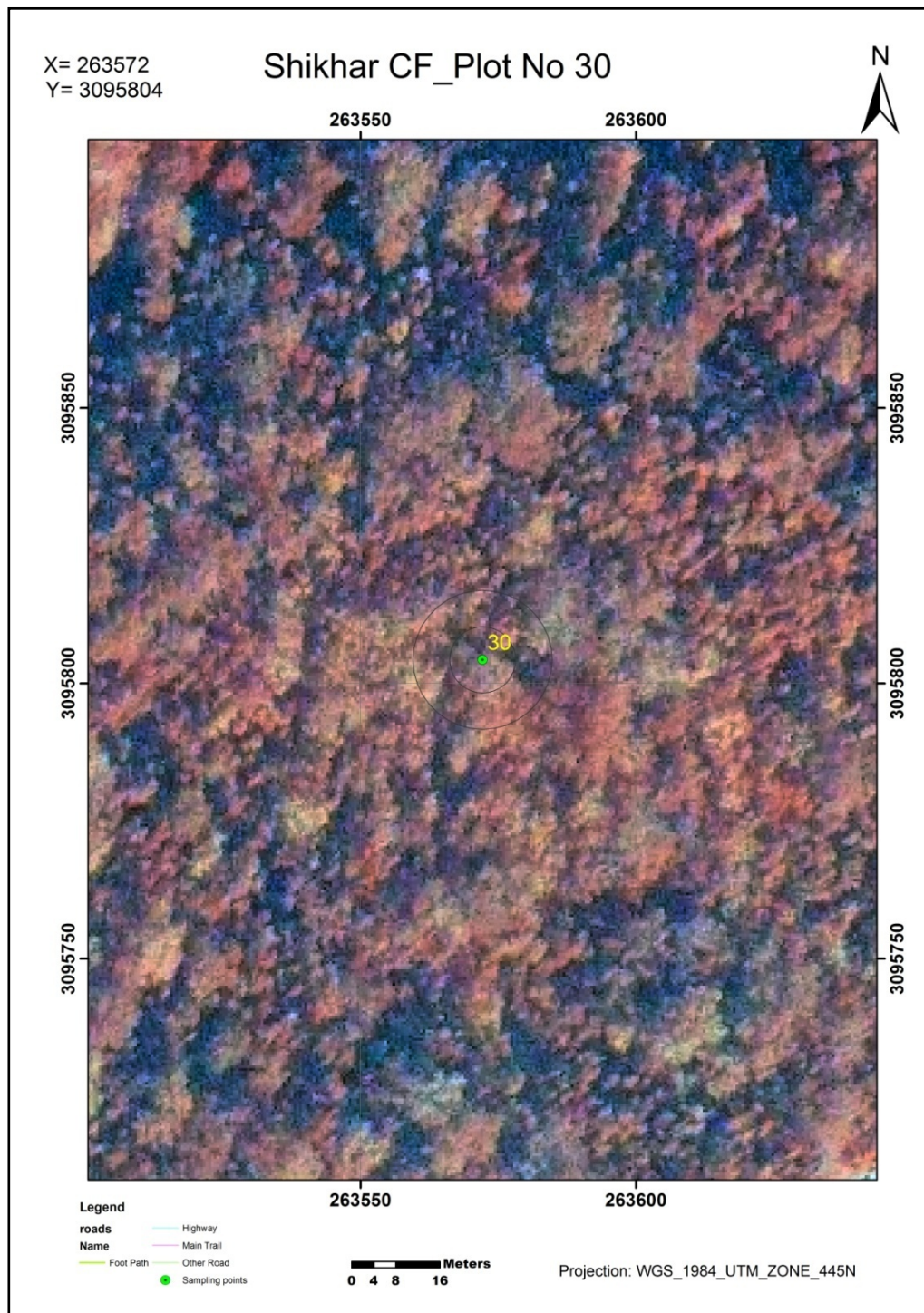
Appendix 3: Details of Digital Camera imagery data acquisition

Image type	RGB image optimized for automatic interpretation.
Format	GeoTIFF with tfw
Compression	Image files non-compressed TIFF.
Source	From digital sensor
View angle	Nadir –looking
Collection procedure	Image files collected during the LiDAR acquisition.
Resolution	0.45 m at 2500 agl altitude
Orthorectification	ortho-rectified to 1 m horizontal precision over the LiDAR
Bands	The image files contain three bands: R, G, and B
R width (app.)	610 - 660nm
G width (app.)	530 - 590nm
B width (app.)	not available
Flight line direction	According to the LiDAR flight plan.
Weather conditions	Obtained with clear weather.
Sun angle	Sun angle must not be less than 40 degrees and, preferably, not more than 80 degrees above horizon during the collect.
Season	In Nepal the photographic months are from October to March. Data taken on March
Projection	UTM zone 45N
Band registration error	Maximum band-to-band dislocation 0.3 pixels
Horizontal location error	Max +/-1m
Tiling	Images are tiled to 12Mb each.
Image Tile index	Ortho_tileindex_Block_Icimod

Appendix 4: Details of LIDAR data acquisition

Customer	Forest Resource Assessment in Nepal, Ministry of Forests and Soil Conservation
Date Flown	20110316 / 20110328 / 20110401 / 20110402
Times of collection (UTC)	02:45 – 08:20 / 03:46 – 05:00 / 04:01 – 05:45 / 03:31 – 05:30
Date Processed	20110530
Projection	UTM
Datum	WGS84
Files included	ASPRS LAS v. 1.2 - 3002 nos.(IC01.las to IV300.las)
Aerial Platform	Helicopter (9N-AIW)
Flying altitude	2200 m AGL
Flying speed	80 knots
Sensor pulse rate	52.9 khz
Sensor Scan speed	20.4 lines/second
Nominal outgoing pulse density @ground level	Average: 0.8 points per square meter
Scan FOW half-angle	20 degrees
Swath @ ground level	1601.47 m
Point spacing	max 1.88 m across, max 2.02 m down
Beam footprint @ ground level	50 cm
Gap file name	No gaps
Tile index file name	tileindex_Block_icomod.dgn

Appendix 5: Enlarged map of the sample plot used for the tree identification in the field



Appendix 6: Data collection Form

Name of Recorder:

Date:

Stratum ID:

Sample Plot

ID:

Bearing from the road		Bearing for the 1st tree from the center of the plot		Plot center	
X		X		X	
Y		Y		Y	
Angle		Angle			

Slope:

Plot radius:

Aspect:

Altitude:

Crown density(%):

S.N	Species	DBH(cm)	CD (m)	Ht (m)	Intermingled tree crowns	Remarks
1						
2						
3						
4						
5						
6						
7						
8						
9						
10						
11						
12						
13						
14						
15						
16						
17						
18						
19						
20						
21						
22						
23						
24						
25						

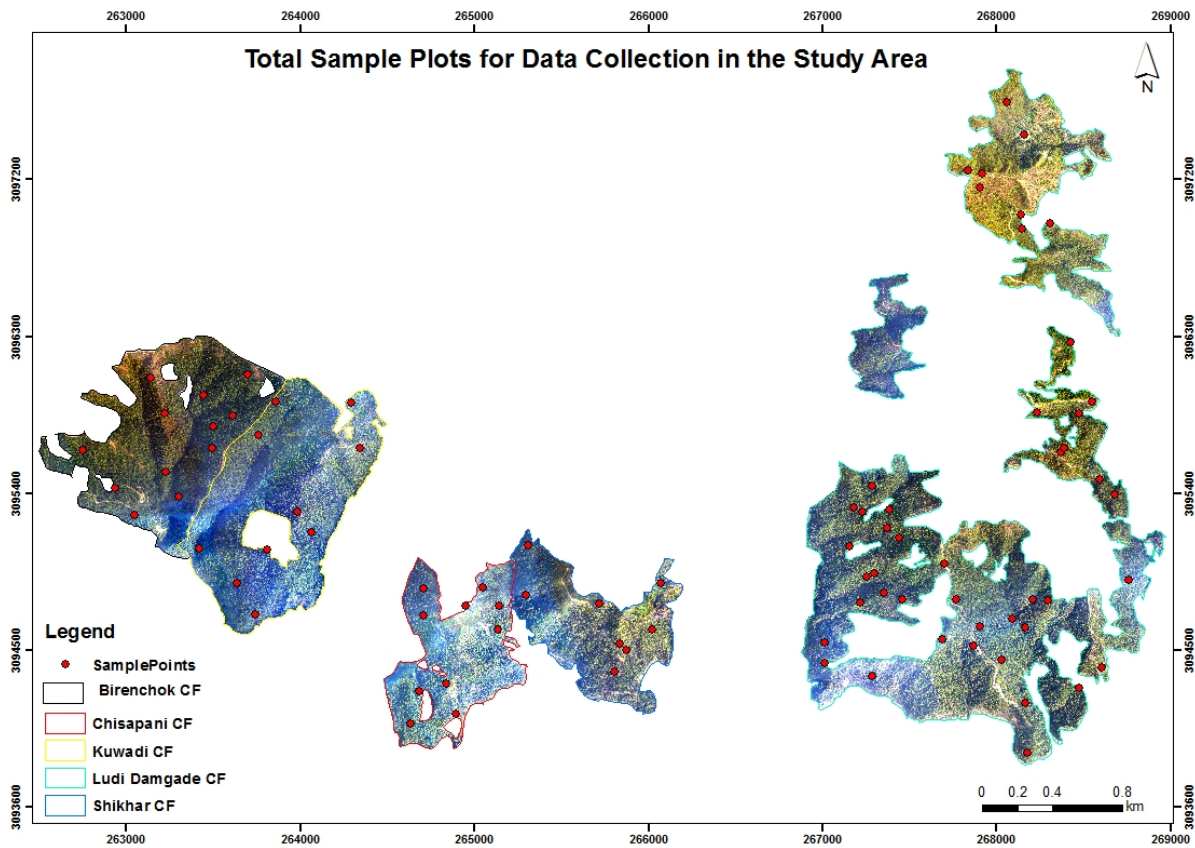
Appendix 7: Slope correction table

Plot size 500m²

Slope%	Radius(m)	Slope%	Radius(m)	Slope%	Radius(m)
0	12.62				
1	12.62	36	13.01	71	13.97
2	12.62	37	13.03	72	14.00
3	12.62	38	13.05	73	14.04
4	12.62	39	13.07	74	14.07
5	12.62	40	13.09	75	14.10
6	12.63	41	13.12	76	14.14
7	12.63	42	13.14	77	14.17
8	12.64	43	13.16	78	14.21
9	12.64	44	13.19	79	14.24
10	12.65	45	13.21	80	14.28
11	12.65	46	13.24	81	14.31
12	12.66	47	13.26	82	14.35
13	12.67	48	13.29	83	14.38
14	12.68	49	13.31	84	14.42
15	12.69	50	13.34	85	14.45
16	12.70	51	13.37	86	14.49
17	12.71	52	13.39	87	14.52
18	12.72	53	13.42	88	14.56
19	12.73	54	13.45	89	14.60
20	12.74	55	13.48	90	14.63
21	12.75	56	13.51	91	14.67
22	12.77	57	13.53	92	14.71
23	12.78	58	13.56	93	14.74
24	12.79	59	13.59	94	14.78
25	12.81	60	13.62	95	14.82
26	12.82	61	13.65	96	14.85
27	12.84	62	13.68	97	14.89
28	12.86	63	13.72	98	14.93
29	12.87	64	13.75	99	14.97
30	12.89	65	13.78	100	15.00
31	12.91	66	13.81	101	15.04
32	12.93	67	13.84	102	15.08
33	12.95	68	13.87	103	15.12
34	12.97	69	13.91	104	15.15
35	12.99	70	13.94	105	15.19

Source: Y.A. Hussin (2001) from lecture note

Appendix 8: Total sample plots for data collection in the study area



Appendix 9: Descriptive statistics of field collected data

DBH (cm)		Height (m)	
Mean	17.92	Mean	12.55
Standard Error	0.16	Standard Error	0.09
Median	15	Median	12.2
Mode	10.5	Mode	10.2
Standard Deviation	8.72	Standard Deviation	5.18
Sample Variance	76.04	Sample Variance	26.8
Range	73	Range	34.3
Minimum	10	Minimum	1
Maximum	83	Maximum	35.3
Sum	50037.7	Sum	35058.5
Count	2793	Count	2793

Appendix 10: ANOVA tests

ANOVA test result of *Shorea robusta* (for relationship between CPA and carbon)

	<i>df</i>	<i>SS</i>	<i>MS</i>	<i>F</i>	<i>Significance F</i>
Regression	1	1909638.61	1909638.61	211.87	4.4776E-29
Residual	130	1171700.61	9013.08		
Total	131	3081339.22			

ANOVA test result of other species (for relationship between CPA and carbon)

	<i>df</i>	<i>SS</i>	<i>MS</i>	<i>F</i>	<i>Significance F</i>
Regression	1	194672.55	194672.55	70.18	9.7967E-11
Residual	45	124826.13	2773.91		
Total	46	319498.68			

ANOVA test result of *Shorea robusta* (for relationship between height and carbon)

	<i>df</i>	<i>SS</i>	<i>MS</i>	<i>F</i>	<i>Significance F</i>
Regression	1	2021005.82	2021005.82	229.18	1.78132E-30
Residual	130	1146385.82	8818.35		
Total	131	3167391.64			

ANOVA test result of other species (for relationship between height and carbon)

	<i>df</i>	<i>SS</i>	<i>MS</i>	<i>F</i>	<i>Significance F</i>
Regression	1	321817.62	321817.62	75.56	3.4589E-11
Residual	45	191650.17	4258.89		
Total	46	513467.79			

ANOVA test result of *Shorea robusta* (for relationship between CPA, height and carbon)

	<i>df</i>	<i>SS</i>	<i>MS</i>	<i>F</i>	<i>Significance F</i>
Regression	2	4633027.72	2316513.86	168.34	1.10025E-36
Residual	129	1775168.44	13761.00		
Total	131	6408196.15			

ANOVA test result of other species (for relationship between CPA, height and carbon)

	<i>df</i>	<i>SS</i>	<i>MS</i>	<i>F</i>	<i>Significance F</i>
Regression	2	502012.3	251006.2	44.30086	2.8832E-11
Residual	44	249301.5	5665.943		
Total	46	751313.8			

Appendix 11: Photos from the field

